Furan-2-ylmethylene Thiazolidinediones as Novel, Potent, and Selective Inhibitors of Phosphoinositide 3-Kinase γ

Vincent Pomel,[†] Jasna Klicic,[†] David Covini,[†] Dennis D. Church,[†] Jeffrey P. Shaw,[†] Karen Roulin,[†] Fabienne Burgat-Charvillon,[†] Delphine Valognes,[†] Montserrat Camps,[‡] Christian Chabert,[‡] Corinne Gillieron,[‡] Bernard Françon,[§] Dominique Perrin,[§] Didier Leroy,[§] Denise Gretener,[§] Anthony Nichols,[§] Pierre Alain Vitte,[#] Susanna Carboni,[#] Christian Rommel,[‡] Matthias K. Schwarz,[†] and Thomas Rückle*,[†]

Departments of Chemistry, Signal Transduction, Biochemical Pharmacology, and Experimental Pharmacology, Serono Pharmaceutical Research Institute, 14 Chemin des Aulx, CH-1228 Plan-les-Ouates, Geneva, Switzerland

Received February 13, 2006

Class I phosphoinositide 3-kinases (PI3Ks), in particular PI3Kγ, have become attractive drug targets for inflammatory and autoimmune diseases. Here, we disclose a novel series of furan-2-ylmethylene thiazolidinediones as selective, ATP-competitive PI3Kγ inhibitors. Structure-based design and X-ray crystallography of complexes formed by inhibitors bound to PI3Kγ identified key pharmacophore features for potency and selectivity. An acidic NH group on the thiazolidinedione moiety and a hydroxy group on the furan-2-yl-phenyl part of the molecule play crucial roles in binding to PI3K and contribute to class IB PI3K selectivity. Compound **26** (AS-252424), a potent and selective small-molecule PI3Kγ inhibitor emerging from these efforts, was further profiled in three different cellular PI3K assays and shown to be selective for class IB PI3K-mediated cellular effects. Oral administration of **26** in a mouse model of acute peritonitis led to a significant reduction of leukocyte recruitment.

Introduction

Phosphoinositide 3-kinases (PI3Ks) are pivotal kinases that participate as lipid, as well as protein, kinases in numerous intracellular signaling pathways. Class I PI3Ks are subdivided into class IA and class IB. Class IA PI3Ks contain p110α, p110β, and p110δ as catalytic subunits, and these are activated in tyrosine kinase receptor signaling. Class IB PI3Ks contain only p110γ as a catalytic subunit, which is mostly activated by seven-transmembrane G-protein-coupled receptors (GPCRs) via its regulatory subunit p101 and G-protein βγ subunits.[1] While PI3Kα and PI3Kβ are ubiquitously expressed, PI3Kγ and PI3Kδ expression is mainly restricted to the hematopoietic system. All four catalytic subunits have been investigated by genetic manipulation. PI3Kα and PI3Kβ knockout (KO) mice revealed early-stage lethality during embryonic development,[2,3] while mice lacking expression or activity of PI3Kγ and PI3Kδ did not exhibit any overt adverse phenotype.[4] PI3Kγ KO mice showed reduced chemoattractant-induced neutrophil migration to infection sites and respiratory burst.[5−8] Furthermore, mast cell degranulation was severely impaired in these genetically modified mice.[9] The aggregate of the genetic studies shows that PI3Kγ plays a crucial role in mediating leukocyte chemotaxis as well as mast cell degranulation, making it a potentially interesting target for autoimmune and inflammatory diseases.[10,11] At the same time, the genetic studies indicate that PI3K isoform selectivity will be a crucial factor determining success or failure of PI3K inhibitor programs on the way to the clinic.

Several PI3K inhibitors are already known, including natural products such as staurosporine, quercetin, myricetin, and wortmannin.[12] Another widely used inhibitor is LY294002,[13] which
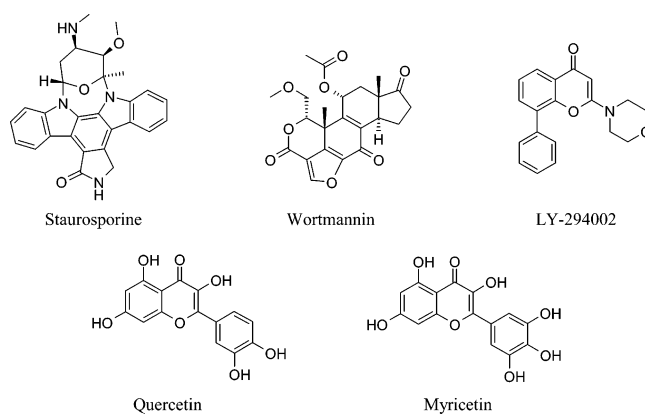

Figure 1. Known PI3K inhibitors.[12,13]

was the first synthetic molecule known to inhibit class I PI3Ks (see Figure 1). The poor biopharmaceutical properties and lack of PI3K isoform selectivity of these first-generation inhibitors have encouraged us, as well as others, to seek PI3Kγ selective inhibitors with more appropriate profiles.[14−29,58] From a structural point of view, the PI3K inhibitors currently in the public domain can be divided into two classes: derivatives of LY294002[30,31] and nonrelated structures. All published structures of inhibitors of the PI3Kγ isoform do not appear to be derivatives of LY294002 (see Figure 2).

This report discusses the discovery of a new chemical series of potent and selective PI3Kγ inhibitors, culminating in the development of compound **26**. The first two molecular generations of this series were presented recently.[10] This article will describe the follow-up program, which had a primary aim to improve PI3K class IB selectivity.

The identification of an initial set of furan-2-ylmethylidene 4-oxo-2-thiothiazolidine or 2,4-dioxothiazolidine (also referred to in the text as rhodanine or thiazolidinedione (TZD), respectively) PI3Kγ inhibitors was achieved using a proprietary substructure analysis method, as described previously.[32,33] Thus, a set of 59 000 compounds was selected from our corporate

---

* To whom correspondence should be addressed. Address: Serono Pharmaceutical Research Institute, Serono International S.A, 14 Chemin des Aulx, CH-1228 Plan-les-Ouates, Geneva, Switzerland. Phone: +41 22 706 9848. Fax: +41 22 706 9565. E-mail: thomas.ruckle@serono.com.
† Department of Chemistry.
‡ Department of Signal Transduction.
§ Department of Biochemical Pharmacology.
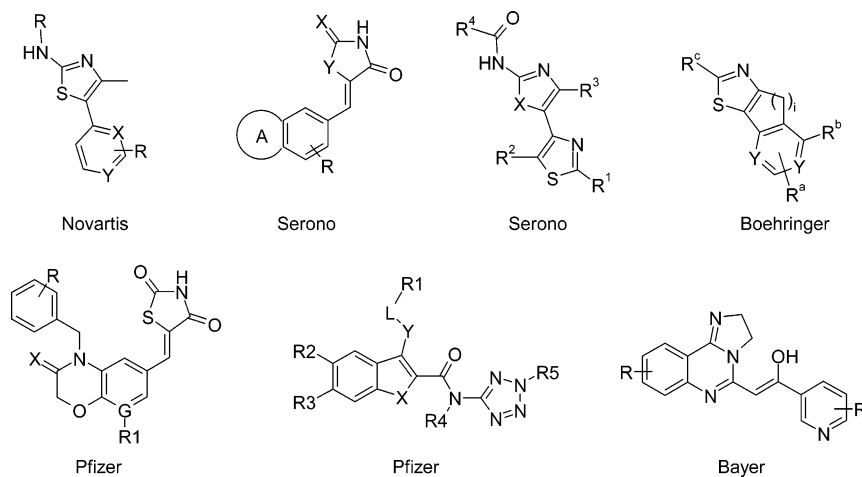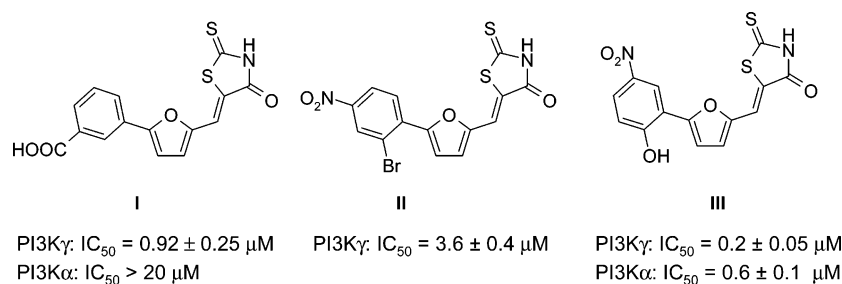# Department of Experimental Pharmacology.

Figure 2. PI3Kγ Inhibitors from patent literature.[14−29,58]

Chart 1. Representative Active Compounds of Initial PI3Kγ High-Throughput Screening

| I	II	III
PI3Kγ: IC$_{50}$ = 0.92 ± 0.25 μM	PI3Kγ: IC$_{50}$ = 3.6 ± 0.4 μM	PI3Kγ: IC$_{50}$ = 0.2 ± 0.05 μM
PI3Kα: IC$_{50}$ > 20 μM		PI3Kα: IC$_{50}$ = 0.6 ± 0.1 μM

compound collection and tested in a high-throughput (HT) PI3Kγ enzyme inhibition assay. This led to the identification of several inhibitors, all of which exhibited only low-micromolar activity. Accordingly, the chemical structures of these compounds were subjected to discrete substructure analysis,[33] which led to the identification of a generic substructure as being the fragment that was most likely to be the basis of the observed inhibitory activity. This substructure was subsequently used for in silico screening of commercial databases, which in turn led to the identification of a number of novel inhibitors whose structures comprised thiazolidinedione or closely related motifs. Among these, furan-2-ylmethylidene 4-oxo-2-thiothiazolidines were particularly prominent (Chart 1), exhibiting IC$_{50}$ values in the 0.9−5 μM range.

After identification of compound **I**, already displaying promising selectivity against PI3Kα, a secondary focused screening campaign involving rhodanine and thiazolidinedione derivatives was carried out to further investigate the structure−activity relationship (SAR). We noticed that rhodanine and thiazolidinedione derivatives bearing the same peripheral substitution pattern were equipotent against PI3Kγ, which encouraged us to base the synthetic medicinal chemistry program exclusively on thiazolidinedione derivatives. The objectives were to (i) increase potency against PI3Kγ, (ii) improve selectivity versus other PI3K isoforms, and ultimately, (iii) develop an orally active molecule with an appropriate biopharmaceutical profile.

We have previously shown that the thiazolidinedione core plays an important role in conferring binding affinity to PI3K.[34] This report, together with another recent one,[35] describes the SAR studies around the Western part, i.e., the heteroarylmethylene moiety, of this class of inhibitors. Thiazolidinediones are well-established modulators of several biological targets, especially known as agonists of peroxisome proliferator-activated receptors (PPARs).[36,37] Several drugs containing a thiazo-

**Chart 2.** Retrosynthetic Analysis Amenable to Parallel Synthesis
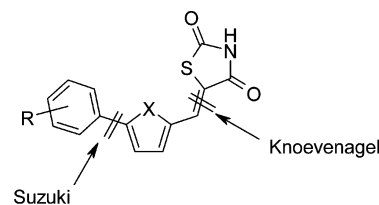
lidinedione as structural motif are on the market as insulin-sensitizers. In consequence, we assessed the binding of our thiazolidinedione series in the early phase of our drug discovery program to various PPAR subtypes (α, γ, δ) . None of our inhibitors tested showed significant activity at concentrations as high as 10 μM.

Results and Discussions

Chemistry. To gain quick access to a range of final molecules for testing against h-PI3Kγ, a simplified parallel synthesis strategy was developed consisting of an initial Suzuki cross-coupling reaction followed by a Knoevenagel reaction, starting from the appropriate furan or thiophene boronic acid derivatives (Chart 2).

In the first campaign, special emphasis was given to the development of a general synthetic route that could be applied to a diverse set of aryl bromides. To cover the whole array of chemical reactivity, two distinct Suzuki coupling procedures were used, as described in procedure A of Scheme 1,[38−41] using toluene/ethanol as solvents, potassium carbonate as base, and tetrakistriphenylphosphine palladium as catalyst, and in procedure B, using water as solvent, potassium carbonate as base, and palladium acetate as catalyst.[42,43]

To access quickly a large number of closely related structures, we did not optimize the Suzuki reaction for high yields and we

Scheme 1. Parallel Synthesis of Furan-2-ylmethylene Thiazolidinediones[a]

[X = S, O]

Intermediates
(**1a - 41a**)

Final Compounds
(**1-41**)
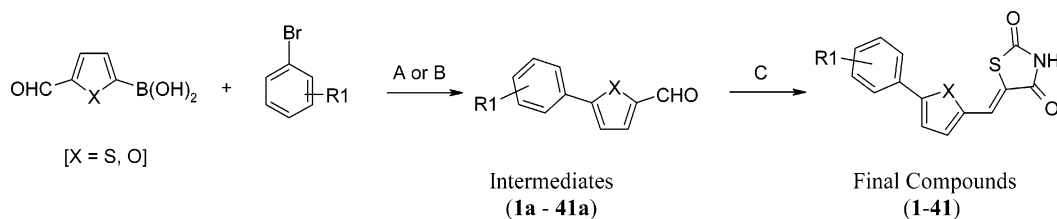
[a] Reagents and conditions: (A) Pd(PPh$_3$)$_4$, K$_2$CO$_3$, toluene/EtOH, Δ; (B) Pd(OAc)$_2$, K$_2$CO$_3$, H$_2$O; (C) thiazolidinedione, β-ala, AcOH, Δ.

Scheme 2. Synthesis of Furan-2-ylmethylene Thiazolidinediones via Protection and Deprotection Steps[a]

26c   **26b**   **26a**   **26**
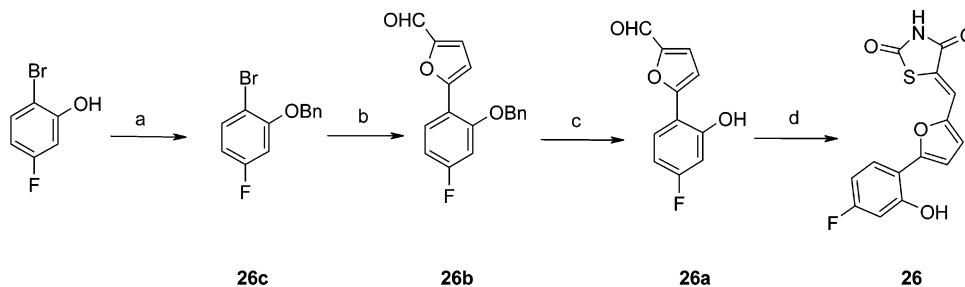
[a] Reagents and conditions: (a) benzylbromide, K$_2$CO$_3$, THF, Δ, 68%; (b) furfuralboronic acid, Pd(PPh$_3$)$_4$, K$_2$CO$_3$, toluene/EtOH, Δ, 56%; (c) BCl$_3$, DCM, −30 °C, 66%; (d) thiazolidinedione, β-ala, AcOH, Δ, 95%.

developed a short workup protocol consisting of a simple filtration through a silica gel pad. The resulting intermediate compounds (**1a**−**41a**), having average purities of 85−95%, were directly used for the next step without further purification.

The Knoevenagel reaction was performed under acidic conditions using 2,4-thiazolidinedione and β-alanine.[44] The advantages of these conditions were numerous: all starting materials were readily soluble; the reaction was quick and clean; the final insoluble compound was precipitated in the course of the reaction, yielding essentially pure final compound (purities >90%). At this stage, the products were fully analyzed and characterized before entering the biological tests.

In parallel, a second synthetic approach was developed amenable to producing multigram quantities required for the later-stage experiments in vivo, in which the yield of the cross-coupling reaction was optimized from 5% to 50−60%. This second approach was based on the protocol used for the parallel synthesis approach (Scheme 1, conditions A), but with an intermediate protection/deprotection sequence of the phenolic hydroxy group, as shown in Scheme 2.

Intermediate **26a** could be accessed over three steps in 25% yield. The phenol group was first protected by a benzyl group and the resulting bromobenzyloxy derivative **26c** was coupled to furfuralboronic acid using a palladium catalyst. Intermediate **26b** was then debenzylated with boron trichloride at −30 °C to afford intermediate **26a**. The improved yield of the Suzuki reaction with protected phenols may be explained by the reduction of the organopalladium intermediate in the presence of free phenols. The Knoevenagel reaction afforded compound **26** in 95% yield with high purity (96%) requiring no further purification. Compounds such as **26** that progressed into in vivo experiments were transformed into the corresponding potassium salts using KOH in THF/water.

Biological Activity. Inhibitory activity against PI3Kγ was determined by measuring the percentage of inhibition at 1 and 10 μM compound concentration as a primary screen. Compounds with percentage of inhibition values (% INH) higher than 50% were progressed into full IC$_{50}$ value determination and, depending on their activity, tested against PI3Kα to determine the selectivity ratio. For selected inhibitors displaying

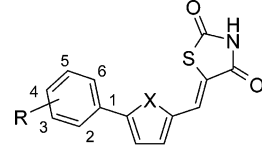**Table 1.** Inhibition of h-PI3Kγ and h-PI3Kα: Phenols

compd	R	method[a]	anal. data[b]	PI3Kγ (nM)[c]	PI3Kα (nM)[c]
1	H	A	a	20000	nd
2	2-OH	A	a	30 ± 5	330 ± 50
3	3-OH	A	a	290 ± 50	1800 ± 300
4	4-OH	A	a	380 ± 70	3600 ± 700

[a] Method A: prepared according to Scheme 1, using conditions A. [b] Analytical data: (a) NMR, LC/MS, mp, CHN, HPLC >90%. [c] All values determined in triplicate. IC$_{50}$ values in nM. nd: not determined.

an interesting enzymatic selectivity profile, cellular activity was assessed, as well as complete class I PI3K enzymatic selectivity (PI3Kα,β,γ,δ), followed in some cases by pharmacological evaluation in vivo.

Early on, we hypothesized that the phenol group was important in conferring PI3K binding, based on an inspection of some of the early compounds (such as **II** and **III**) and our previously gained insights into the binding mode of this type of inhibitors.[10,34,35] The first series of compounds was made to test this hypothesis and to probe how the position of the phenolic hydroxyl group would affect the activity. The results, summarized in Table 1, confirmed the importance of the phenolic hydroxy group for PI3K inhibition (**1** vs **2**). Repositioning the hydroxy group around the phenyl ring from position 2 to positions 3 and 4 resulted in a 10-fold reduction of the activity. Interestingly, the 10-fold selectivity for PI3Kγ versus PI3Kα was retained between the three regioisomers, encouraging us to consider substitutions in all three positions in the design of a follow-up library.

Because it became apparent that the interaction of the hydroxy group, probably via hydrogen bonding to an appropriate residue in the enzyme, is crucial for PI3Kγ inhibition, we decided to explore substituents other than hydroxy to probe what effects the hydrogen-bonding capacity, charge, polarity, and size of a substituent would have on PI3K binding. The goal was to retain or improve the inhibitory potency against PI3Kγ and, at the

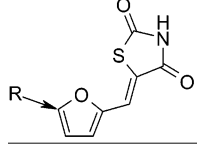**Table 2.** Inhibition of h-PI3Kγ: 2- and 3-Substituted Phenylfurans

compd	X	R	method[a]	anal. data[b]	PI3Kγ (nM)[c]
5	O	2-OMe	A	a	44% INH
6	O	2-Cl	A	a	20000
7	O	2-F	A	a	1200 ± 330
8	O	2-CO_2H	A	a	4% INH
9	O	2-CO_2Me	A	a	2% INH
10	O	2-CH_2−CO_2H	A	a	12% INH
11	O	3-CO_2H	A	a	4300 ± 170
12	O	3-CO_2Me	A	a	13500 ± 1500
13	O	3-CH_2−CO_2H	A	a	15% INH
14	O	2-NHAc	A	a	24% INH
15	O	2-NH_2−5-NO_2	A	b	18% INH
16	S	2-OH	A	a	27% INH
17	O	3-OMe	A	a	2600 ± 470
18	O	3-NO_2	A	a	24% INH
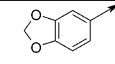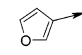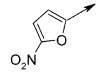
[a] Method A: prepared according to Scheme 1, conditions A. [b] Analytical data: (a) NMR, LC/MS, mp, CHN, HPLC >90%; (b) LC/MS, HPLC >90%. [c] All values determined in triplicate. IC$_{50}$ values in nM. % INH at 1 μM (INH = inhibition).

same time, to maximize the selectivity against the other PI3K isoforms. The results are summarized in Table 2.

Replacement of the 2-hydroxy group with small, polar substituents with limited hydrogen-bond acceptor potential led to significant reduction in activity (**5**−**7**). Repositioning the methoxy group to position 3 did not lead to any improvement in terms of activity (**17**). Similarly, substitution with larger polar or charged groups (as in **8**−**10**) caused a marked loss in activity. The same set of substituents in position 3 produced compounds with similarly low activities (**11**−**13**), as did the introduction of a nitro group at the same position (**18**). Interestingly, when the 2-hydroxy group was replaced by hydrogen-bond-donating (but not hydrogen-bond-accepting) NH groups at the same 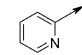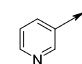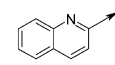position (**14**, **15**), no significant inhibition of PI3Kγ activity was observed at 1 μM. From the above data, we inferred that a small group capable of acting as a hydrogen-bond acceptor and donor in position 2, and, to a lower extent, also in positions 3 and 4 is crucial for a strong interaction with the PI3Kγ binding site. The importance of geometry and size is demonstrated by the binding data of compound **16**, where the central furan ring is replaced by a thiophene, shifting the 2-hydroxy group away from its optimal position in the protein-binding pocket (see section Docking Studies and X-ray Crystallography). None of the compounds shown in Table 2 (**5**−**18**) exhibited any inhibitory activity against PI3Kα at concentrations up to 20 μM.

Next, we explored a set of mono- and bicyclic heterocycles containing oxygen or nitrogen atoms capable of functioning as a hydrogen-bond acceptor, the results of which are summarized in Table 3. In the case of oxygen-containing heterocycles, both piperonyl and furan derivatives (**19**−**21**) showed reduced activity probably because of steric hindrance and/or suboptimal positioning of the hydrogen-bond-accepting oxygen. On the other hand, the 2- and 3-pyridine analogues (**22** and **23**, respectively) maintained activities in the same range as the respective phenol compounds (**2** and **3**, respectively), with a mere 3-fold loss in IC$_{50}$ values (30 vs 110 nM; 290 vs 950 nM). Nonetheless, the total lack of selectivity observed for both 2- and 3-pyridines suggests a special role of the hydroxy group in differential binding to PI3Kγ and PI3Kα isoforms. However, introduction of larger pyridine analogues, such as 2-quinoline and 8-quinoline (**24** and **25**, respectively), was no longer tolerated by the enzyme. The reduced activity may possibly be explained by increased

Table 3. Inhibition of h-PI3Kγ and h-PI3Kα: Heteroaryl-Substituted Furans

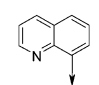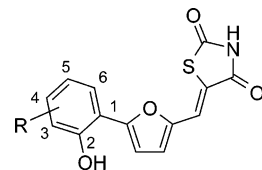| Compd	R	method[c]	anal.data[d]	PI3Kγ •[nM][e]	PI3Kα [nM][e]
19		A	a	20000	20000
20		B	a	840 ± 140	nd
21		B	a	20000	nd
22		A	a	110 ± 20	185 ± 40
23		A	a	950 ± 310	630 ± 70
24		A	a	13%INH	nd
25		A	a	17%INH	nd

[a] Method A: prepared according to Scheme 1, condition A. Method B: prepared according to Scheme 1, condition B. [b] Analytical data: (a) NMR, LC/MS, mp, CHN, HPLC >90%; (b) LC/MS, HPLC >90%. [c] All values determined in triplicate. IC$_{50}$ values in nM. % INH at 1 μM (INH = inhibition). nd: not determined.

steric hindrance and/or by a poor positioning of the heterocyclic nitrogen atom, preventing proper hydrogen bonding with the enzyme.

Having thus established the importance of the 2-hydroxy group for both potency and isoform selectivity, we set out to explore the effects of additional substituents on those two key parameters (see Table 4).

The introduction of a second substituent was found to have little influence on the inhibition of PI3Kγ (all IC$_{50}$ values in the range 20−80 nM), with the only exception being the carboxylate group in position 5 (compound **36**), which significantly reduced the activity. One explanation offered by the inspection of the cocrystal structure argues that the carboxylate group is positioned close to the Lys890 side chain, with which it can form an ionic interaction. This stabilization of the negative charge will increase the polarization of the π electron system and lower the electron density of the 2-hydroxy through the long-range resonance effect, thus reducing its effectiveness as a hydrogen-bond acceptor. Furthermore, because of the interaction between Lys890 and the carboxylate, **36** may slightly be shifted, potentially resulting in weaker binding (for more details, consult section Docking Studies and X-ray Crystallography).

In contrast to the potency against the PI3Kγ isoform, the PI3Kγ/α selectivity ratio was found to depend considerably on the nature and the position of the second substituents, ranging from 13-fold (for **33**) to 30-fold (for **26**). Among the compounds with markedly reduced activity against PI3Kα (IC$_{50}$ > 1 μM) are compounds **35** and **36**. It is interesting to note that,

Table 4. Inhibition of h-PI3Kγ and h-PI3Kα: Substituted 2-Furan-2-ylphenols

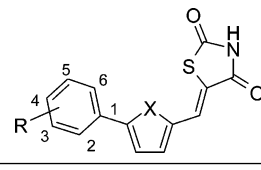| compd	R	method[a]	anal. data[b]	PI3Kγ (nM)[c]	PI3Kα (nM)[c]	pK_a[d]
2	4-H	A	a	30 ± 5	330 ± 50	9.5 ± 0.1
26	4-F	C	a	33 ± 10	935 ± 150	8.4 ± 0.1
27	4-OH	B	a	20 ± 8	190 ± 20	8.7 ± 0.1
28	4-CO$_2$Me	B	a	29 ± 5	210 ± 25	8.7 ± 0.1
29	5-F	B	b	37 ± 10	455 ± 50	9.1 ± 0.1
30	5-Cl	B	a	43 ± 5	545 ± 75	8.9 ± 0.1
31	5-CN	B	a	40 ± 10	220 ± 40	7.3 ± 0.1
32	5-OCF$_3$	B	a	56 ± 20	600 ± 40	8.7 ± 0.1
33	5-Me	B	a	39 ± 6	500 ± 70	9.7 ± 0.1
34	5-OH	B	a	20 ± 3	100 ± 10	10^e
35	3-NO$_2$	B	b	80 ± 20	1250 ± 250	6.6^e
36	5-CO$_2$H	B	b	530 ± 30	1350 ± 150	8.6 ± 0.1

^{a} Method A: prepared according to Scheme 1, condition A. Method B: prepared according to Scheme 1, condition B. Method C: prepared according to Scheme 2. ^{b} QC/analytical data. (a) NMR, LC/MS, mp, CHN, HPLC >90%. (b) LC/MS, HPLC >90%. ^{c} All values determined in triplicate. IC$_{50}$ values in nM. % INH at 1 μM (INH = inhibition). nd: not determined. ^{d} Experimental pK_a values. ^{e} Predicted pK_a values (ACD software, version 7.0).

considering that Lys890 in PI3Kγ is replaced by neutral Gln859 in PI3Kα and hence has no possibility for ionic interaction of the 5-carboxylate in **36**, the adverse effect of this group on the hydrogen-bonding capability of 2-hydroxy is somewhat diminished, resulting in the lowest α/γ selectivity among all 2-hydroxy analogues tested. Another compound showing reduced potency on PI3Kα (but constant activity against PI3Kγ) is the 4-fluoro derivative **26**. Detailed inspection reveals that the replacement of the hydroxy group by a fluoro atom in either the 4- or the 5-position (**27** vs **26**; **34** vs **29**) leads to reduced activity on PI3Kα. A possible reason could be reduced fluorine hydration of these solvent-exposed groups. However, while this effect is less prominent for the more tightly binding PI3Kγ isoform (roughly 2-fold), it leads to a 5-fold difference in binding to the less optimal ATP^a binding site of PI3Kα, resulting overall in an increased PI3Kγ/PI3Kα selectivity.

In an attempt to rationalize the influence of additional substituents in the series of compounds shown in Table 4, we asked whether the inhibitory potency against PI3Kγ and/or the PI3Kα/PI3Kγ selectivity would depend on the acidity of the phenolic hydroxy group, the underlying hypothesis being that with increasing acidity, the electron density on the oxygen atom will decrease, hence weakening its hydrogen-bond-forming capacity. The panel of 4- and 5-substituted 2-phenol derivatives presented in Table 4 covers a pK_a range from 7 to 10 for the phenolic hydroxy group. Although we could observe a weak tentative correlation between PI3Kγ inhibition (log IC$_{50}$) and pK_a values ($R^2 = 0.6$), no significant correlation was observed for PI3Kα and hence the selectivity ratio.

Finally, a highly focused set of analogues of compound **26** was prepared, the results of which are summarized in Table 5.

Corroborating previous results, replacing the 2-hydroxy by a methoxy group, while maintaining the fluorine in the 4-position (compound **37**), led to a significant reduction of the activity against PI3Kγ. This confirms that the hydroxy group functions

^{a} Abbreviations: ATP, adenosine triphosphate; HBD, hydrogen-bond donor; HBA, hydrogen-bond acceptor; PKB, protein kinase B; SCF, stem cell factor; MCP-1, monocyte chemotactic protein-1; CCR, chemokine receptor; CSF-1, colony stimulating factor 1.

Table 5. Inhibition of h-PI3Kγ and h-PI3Kα: Fluorine Substituted 2-Furan-2-ylphenols

compd	X	R	method[a]	anal. data[b]	PI3Kγ (nM)[c]	PI3Kα (nM)[c]
26	O	2-OH, 4-F	C	a	33 ± 10	935 ± 150
37	O	2-OMe, 4-F	A	a	11% INH	nd
38	S	2-OH, 4-F	A	a	4% INH	nd
39	O	4-OH, 2-F	B	a	260 ± 30	1000 ± 70
40	O	2F, 4-F	A	a	3800 ± 420	nd
41	O	2-OH, 3-F 5-F	B	a	29 ± 3	340 ± 25

^{a} Method A: prepared according to Scheme 1, condition A. Method B: prepared according to Scheme 1, condition B. Method C: prepared according to Scheme 2. ^{b} QC/analytical data: (a) NMR, LC/MS, mp, CHN, HPLC >90%. ^{c} All values determined in triplicate. IC$_{50}$ values in nM. % INH at 1 μM (INH = inhibition). nd: not determined.

as a hydrogen-bond donor and hydrogen-bond acceptor in the present molecular context and/or that space is limited to accommodate only a hydrogen group. Substitution of the 2-hydroxy group by fluorine produced a weak inhibitor, **40** (IC$_{50}$ = 4 μM), with activity comparable to activities of other compounds lacking the phenolic hydroxy group (see Table 2). Switching the positions of the hydroxy group and the fluorine atom resulted in a compound with similar activity (**39**) as the corresponding nonfluorinated analogue **4** (see Table 1). Replacement of the 4-fluoro by a 3,5-difluoro substitution pattern (compounds **26** and **41**) maintained the activity against PI3Kγ but decreased the selectivity against PI3Kα. Together with a similar result obtained from the 5-fluoro analogue **29** (see Table 4), this indicates that the beneficial influence of the 4-fluoro substituent on the isoform selectivity is probably not only due to σ-inductive effects but must depend on additional factors. Of note, replacement of the central furan by a thiophene produced an inactive compound (**38**), as previously seen for compounds **2** and **16** (see Table 2 and section Docking Studies and X-ray Crystallography).

In summary, the SAR information obtained from the compounds presented here indicates that the 2-hydroxy group plays a crucial role in conferring PI3K binding and inhibition, probably through a bidentate HBA/HBD function, leading to PI3Kγ inhibitory activities in the range 30–50 nM. Addition of other substituents around the 2-hydroxyphenyl moiety has no major influence on the inhibitory potency. However, introduction of a fluorine atom specifically at the 4-position leads to a notable increase in selectivity against PI3Kα. Modeling studies suggest that the fluorine atom at C-4 is located in the proximity of a nonconserved area of the binding site, where the nonpolar Ala885 (present in PI3Kγ) is replaced by the polar Ser606 (present in PI3Kα). This could account for the increased isoform selectivity. Whether this hypothesis holds up and hence enables medicinal chemists to design even more selective PI3Kγ inhibitors in a rational way remains an open question. An alternative hypothesis argues that the plasticity of the class IA and class IB PI3K isoforms is different, in which case the shape of the ATP-binding site would matter less than flexibility and adaptability upon inhibitor binding. This would render rational design of selective PI3Kγ inhibitors more complex. Further work is required to shed more light on the key molecular interactions between PI3Ks and small-molecule inhibitors that determine isoform selectivity.

Table 6. Class I PI3K Selectivity Profile for Compounds **26** and **2** in Comparison with Wortmannin and LY294002

| PI3K | IC$_{50}$ (nM)^a | | | |
	α	β	γ	δ
Wortmannin	1 ± 0.2	10 ± 2	5 ± 1	9 ± 2
LY294002	720 ± 200	306 ± 40	7260 ± 2600	1330 ± 260
2	330 ± 50	20000	30 ± 5	> 5000
26	940 ± 150	20000	30 ± 10	20000

^{a} All values determined at least in triplicate.

Table 7. Selectivity Profile of Compound **26** against 80 Protein Kinases^a

protein kinase	remaining enzymatic activity of **26** (% of control)	protein kinase	remaining enzymatic activity of **26** (% of control)
Abl(h)	92	MEK1(h)	96
AMPK(r)	90	MKK4(m)	85
Arg(m)	85	MKK6(h)	105
Aurora-A(h)	85	MKK7β(h)	2 ($>10\,\mu M^b$)
Axl(h)	74	MSK1(h)	72
Blk(m)	70	p70S6K(h)	190
Bmx(h)	102	PAK2(h)	178
CaMKII(r)	97	PDGFRα(h)	85
CaMKIV(h)	111	PDGFRβ(h)	96
CDK1/cyclinB(h)	80	PDK1(h)	104
CDK2/cyclinA(h)	84	PI3Kγ(h)	5 (20 nM^b)
CDK2/cyclinE(h)	93	PKA(h)	89
CDK3/cyclinE(h)	117	PKBα(h)	97
CDK5/p35(h)	83	PKBβ(h)	103
CDK6/cyclinD3(h)	89	PKBγ(h)	96
CDK7/cyclinH/MAT1(h)	77	PKCα(h)	98
CHK1(h)	94	PKCβII(h)	98
CHK2(h)	82	PKCγ(h)	107
CK1(y)	88	PKCδ(h)	109
CK2(h)	6 (20 nM^b)	PKCϵ(h)	93
c-RAF(h)	99	PKCη(h)	91
CSK(h)	103	PKCι(h)	84
cSRC(h)	66	PKCμ(h)	98
Fes(h)	90	PKCθ(h)	102
FGFR3(h)	121	PKD2(h)	91
Flt3(h)	93	PRAK(h)	95
Fyn(h)	91	PRK2(h)	95
GSK3α(h)	66	ROCK$-$II(h)	90
GSK3β(h)	84	Rsk1(h)	104
IGF-1R(h)	96	Rsk2(h)	86
IKKα(h)	82	Rsk3(h)	73
IKKβ(h)	89	SAPK2a(h)	84
IR(h)	90	SAPK2b(h)	89
JNK1α1(h)	97	SAPK3(h)	93
JNK2α2(h)	97	SAPK4(h)	93
JNK3(h)	86	SGK(h)	98
Lck(h)	104	Syk(h)	93
Lyn(h)	101	TrkB(h)	98
MAPK1(h)	103	Yes(h)	99
MAPKAP$-$K2(h)	117	ZAP-70(h)	159

^{a} Protein kinases were assayed with 10 μM of **26** in the presence of 10 μM of ATP. ^{b} IC$_{50}$ value on the enzyme.

Throughout the entire project, the PI3Kγ/PI3Kα selectivity was routinely monitored for all compounds, while the inhibition

of the other class IA PI3K members was only checked for a few key compounds. As an illustration, Table 6 shows the entire class I PI3K selectivity profile for compounds **2** and **26**, emphasizing the excellent isoform selectivity of the latter compound. In addition to the selectivity profile for PI3Kγ vs class IA PI3Ks, another important feature of this class of compounds was found to be their excellent selectivity profile against a large set of unrelated protein kinases. As an example, compound **26** was screened against 80 different Ser/Thr and Tyr kinases and shown not to significantly inhibit any of them at 10 μM except for casein kinase 2 (see Table 7).

Docking Studies and X-ray Crystallography. To better understand the interactions of furan thiazolidinedione PI3Kγ inhibitors with the target protein, we determined the crystallographic structure of complexes between PI3Kγ and several representative ligands at resolutions between 2.7 and 2.9 Å. The unequivocal electron density at the ATP-binding site of the protein clearly identified the binding mode of these furan thiazolidinediones (Figure 3). In the case of **26** (Figures 3 and 4), the thiazolidinedione nitrogen, which is expected to be deprotonated, forms a strong salt-bridge interaction with the positively charged Lys833 side chain (2.5 Å), which itself also forms another salt bridge with the side chain of Asp964 (2.8 Å). The 2-hydroxy group on the phenol ring acts as an important hydrogen-bond acceptor by interacting with the backbone NH of Val882 (2.5 Å), while the phenyl and furan rings form hydrophobic interactions with several hydrophobic residues in the active site.

The crystallographic structure of the complex between PI3Kγ and **2** (Figure 5a) was used to carry out molecular modeling by docking, minimization, and induced-fit docking, which provided additional information concerning the interaction of analogues from this series with PI3Kγ and rationalizing the structure$-$activity relationship.

As an example, we present here a model of **4** bound to PI3Kγ, which was generated via induced-fit docking (Figure 5b). This protocol includes sampling of the conformation space of amino acid side chains surrounding the bound inhibitor before redocking of the inhibitor to the newly generated protein conformation. Molecule **4** adopts the same binding mode as **2**, forming an ionic interaction with Lys833 and a lipophilic interaction between benzene and furan rings and the cavity lined by hydrophobic residues Trp812, Ile831, Ile881, Met953, and Phe961. However, the different position of the hydroxy group prevents it from interacting with the buried Val882 backbone NH. Instead, a hydrogen bond with the Ala885 carbonyl oxygen can be formed. Given that both groups are solvent-exposed, the

(a)

(b)
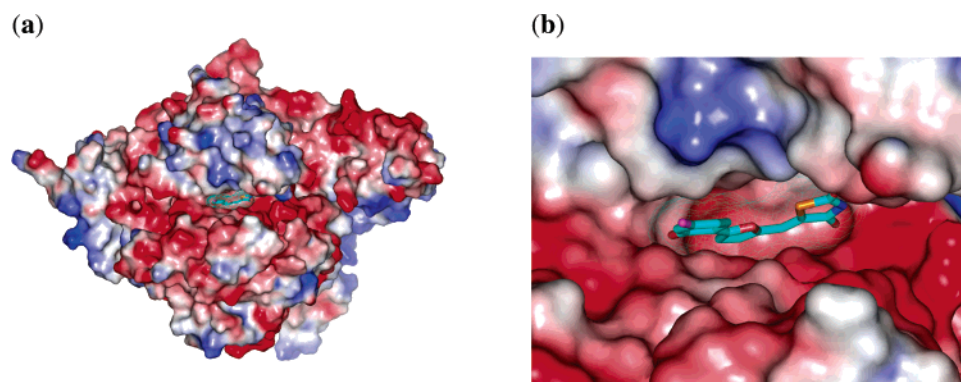
Figure 3. (a) Crystallographic structure of PI3Kγ with the calculated surface electrostatic potential (positive charge shown in blue and negative charge in red), showing the location and size of the binding site of **26**. (b) Close-up of the structure of the active site and binding pocket of **26**.
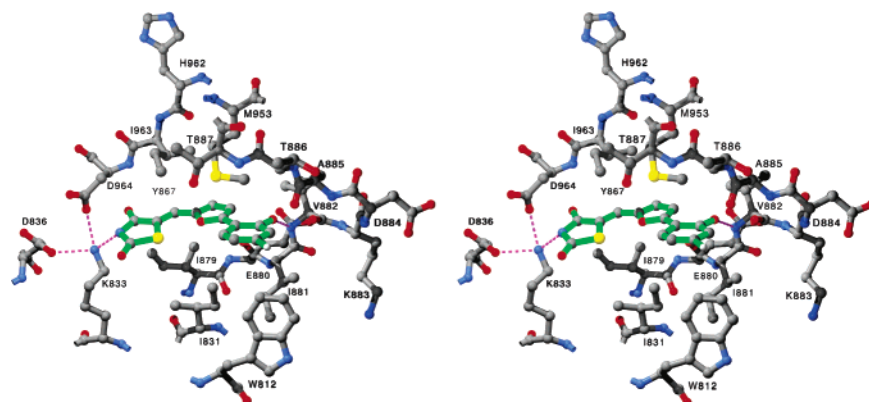
Figure 4. Stereodiagram depicting the crystallographic structure of **26** bound to the active site of human PI3Kγ.
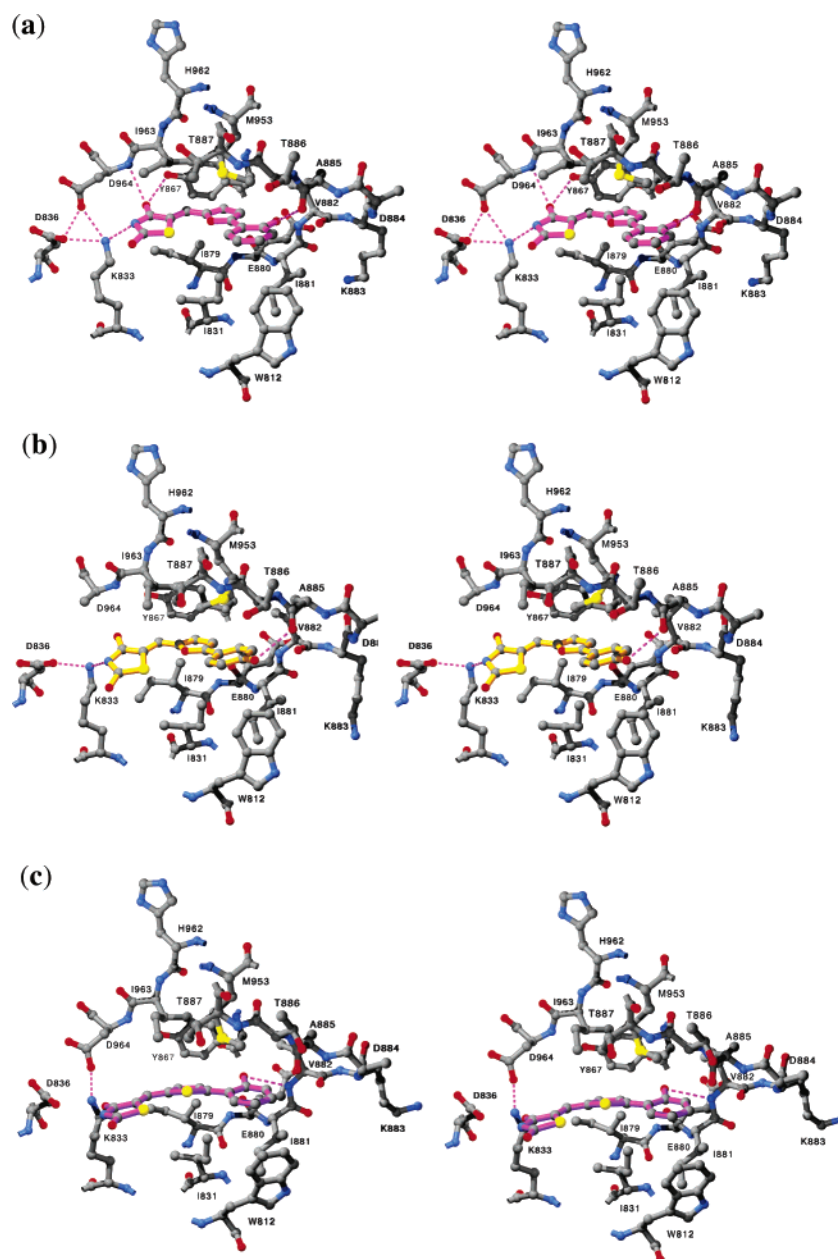

Figure 5. Stereodiagram depicting the crystallographic structure of **2** bound to the active site of human PI3Kγ (a) and stereodiagrams depicting the active site of PI3Kγ with the optimized docked pose of **4** (b) and **16** (c).

stabilizing contribution of this interaction is reduced in comparison with a hydrogen bond to Val882, resulting in a roughly 10-fold drop in potency relative to **2**.

Another example is the model of the thiophene analogue **16** bound to PI3Kγ, which was generated by additional geometry minimization of the docked structure (Figure 5c). Compound

Table 8. Cellular Activity in Raw-264 Murine Macrophages

compd	PI3Kγ (nM)[a]	C5a-mediated PKB/Akt phosphorylation in Raw-264 macrophages (μM)[b]
LY294002	7260 ± 2600	10.0 ± 0.5
26	30 ± 10	0.23 ± 0.08
2	30 ± 5	0.81 ± 0.25
22	110 ± 20	3.65 ± 1.75
27	20 ± 8	3.49 ± 0.09
29	37 ± 10	1.71 ± 0.38
41	29 ± 3	1.39 ± 0.26
28	29 ± 5	0.72 ± 0.25
32	56 ± 20	0.88 ± 0.04
33	39 ± 6	1.06 ± 0.45

[a] IC$_{50}$ values on the isolated enzyme.[54] [b] All values determined at least in triplicate.

16 is almost 1 Å longer along its phenol thiazolidinedione axis and has a more linear shape than the corresponding furane compound **2**. Compared to the binding mode of **2**, **16** is pivoted around the phenol ring and moved toward the outside of the binding pocket in order to retain the hydrogen bond between 2-hydroxy and Val882 NH. As a result, the thiazolidinedione group is displaced by 5 Å and it forms weakened Coulomb interactions within the phosphate-binding site. In addition, the thiophene ring is also significantly displaced from the hydrophobic binding pocket, leading to suboptimal interactions. This example illustrates how the increase in the molecular size when going from furan to thiophene can have as a consequence a drastic reduction in potency.

Cell-Signaling Effects. We further investigated the cellular potency, selectivity, and functionality of our PI3Kγ inhibitors, using cellular assays previously described.[10] In contrast to the class IA PI3Kα, PI3Kβ, and PI3Kδ isoforms, class IB PI3Kγ signals in response to the activation of G$_{\alpha i}$-protein-coupled receptors (GPCRs), including chemokine receptors or receptors for the chemoattractants fMLP or complement 5a (C5a), leading to the generation of phosphatidylinositol-3,4,5-triphosphate (PtdIns(3,4,5)P$_3$) and consequent phosphorylation of PKB/Akt.[6,45] On the basis of, we investigated the effect of our compounds on C5a-mediated PKB/Akt phosphorylation in Raw-264 murine macrophages. This assay was considered a primary cellular filter and allowed us to assess the potency of this inhibitor class on inhibition of PI3Kγ in cells. Compounds inhibited C5a-mediated PKB/Akt phosphorylation in a concentration-dependent manner with submicromolar or low-micromolar IC$_{50}$ values (Table 8). As an illustration, Figure 6 shows a dose response curve obtained for compound **26** in comparison to LY294002.

To validate the selective inhibition of PI3Kγ, as opposed to unselective effects on PI3Kδ or PI3Kα/PI3Kβ activities at a cellular level, we further selected the most potent and selective inhibitors to compare their effects on cellular readouts specific to PI3Kγ, PI3Kδ, or PI3Kα/PI3Kβ signaling. As described, class IA PI3Ks signal downstream of cytokine and growth factor receptors. Activation of primary mast cells with SCF, the ligand for the receptor tyrosine kinase c-kit, is mediated exclusively by PI3Kδ, and in mast cells isolated from p110d$_{D910A/D910A}$ mutant mice, SCF-induced PKB/Akt phosphorylation is completely abrogated.[46] Encouragingly and in accordance with its in vitro selectivity, compound **26** had no effect on SCF-induced phosphorylation of PKB/Akt in bone marrow derived mast cells, even at concentrations as high as 10 μM, confirming its lack of activity on the PI3Kδ isoform (Figure 7, full symbols). As a control, we used a reference compound derived from a pyrimidinones series as described previously that selectively inhibits
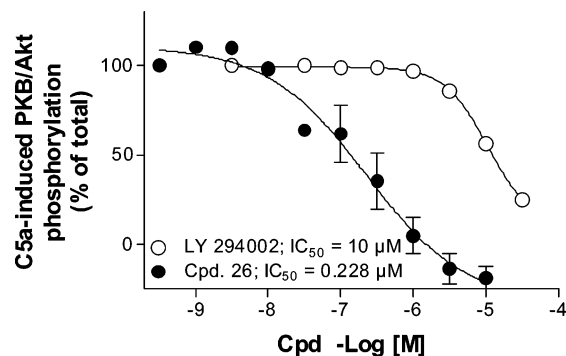
Figure 6. Inhibition of C5a-induced PKB/Akt phosphorylation. After starvation and 30 min of pretreatment with the indicated concentrations of **26** or LY294002, Raw-264 macrophages were activated with 50 nM of C5a for 5 min. PKB/Akt phosphorylation was determined using a phospho-Ser-473 Akt specific antibody, and ELISA protocols, as described in the section Biological Methods. The graph represents the mean ± standard deviation of four independent experiments done in triplicate.
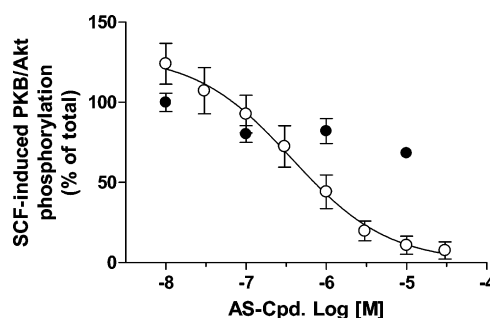
Figure 7. Lack of inhibition of SCF-induced PKB/Akt phosphorylation in mast cells by **26**. After pretreatment with the indicated concentrations of compound, primary mast cells derived from wild-type bone marrow were activated with SCF as described in the section Biological Methods, and PKB/Akt phosphorylation was determined by FACS using phospho-Ser-473 Akt specific antibodies: (closed symbols) **26**; (open symbols) PI3Kδ selective reference.[57]

PI3Kδ (Figure 7, empty symbols).[57] LY294002 abrogated completely SCF-induced Akt phosphorylation at concentrations as high as 20 μM.

To further assess the selectivity of those compounds for class IB PI3Kγ, we examined the capability of **26** and **2** to inhibit preferentially chemokine-induced (PI3Kγ-mediated) but not cytokine-induced (class IA PI3K-mediated) PKB/Akt phosphorylation in the human monocytic cell line THP-1.[10] In those cells, MCP-1, binding to the GPCR chemokine receptor CCR2, strongly induced phosphorylation of PKB/Akt, which was effectively inhibited by **26** at IC$_{50}$ values as low as 0.4 μM (Figure 8). In contrast, induction of PKB/Akt phosphorylation by colony stimulating factor (CSF-1), binding to the growth factor receptor c-fms, was only blocked by **26** at IC$_{50}$ values as high as 4.7 μM (Figure 8). These data are consistent with the in vitro selectivity profile of this inhibitor class, and in particular for compound **26**. None of the inhibitors tested showed any effect on cell viability. LY294002, as an example of a nonselective class I PI3K inhibitor, did not display, as expected, any preferential inhibition in cells.

Cell-Functional Effects. Since chemokine-induced migration of neutrophils, monocytes, and macrophages is, at least in part, a PI3Kγ-dependent mechanism,[5,6,47–49] the effects of blocking PI3Kγ activity on MCP-1-induced chemotaxis in the THP-1 monocytic cell line and in primary mouse monocytes were examined. Compound **26** inhibited MCP-1-mediated chemotaxis in wild-type primary monocytes in a concentration-dependent
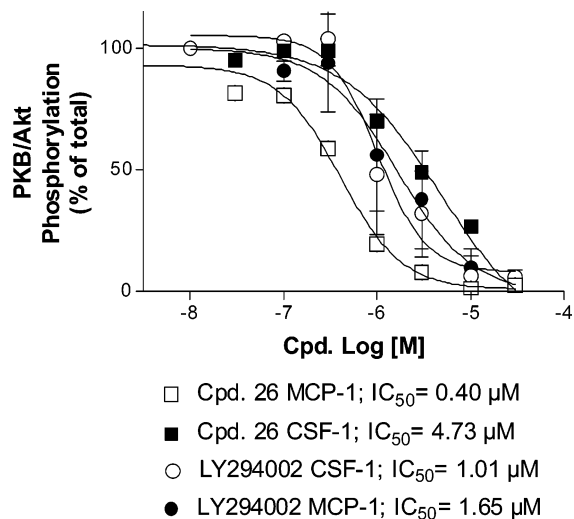
Figure 8. Preferential inhibition of MCP-1- over CSF-1-induced PKP/Akt phosphorylation in cells. After starvation and 20 min of pretreatment with the indicated concentrations of **26** (squares) or LY294002 (circles), THP-1 monocytes were activated by MCP-1 (closed symbols) or CSF-1 (open symbols) and PKB/Akt phosphorylation was monitored by Western blot using phospho-Ser-473 and wild-type specific Akt antibodies and quantified as described in the section Biological Methods.
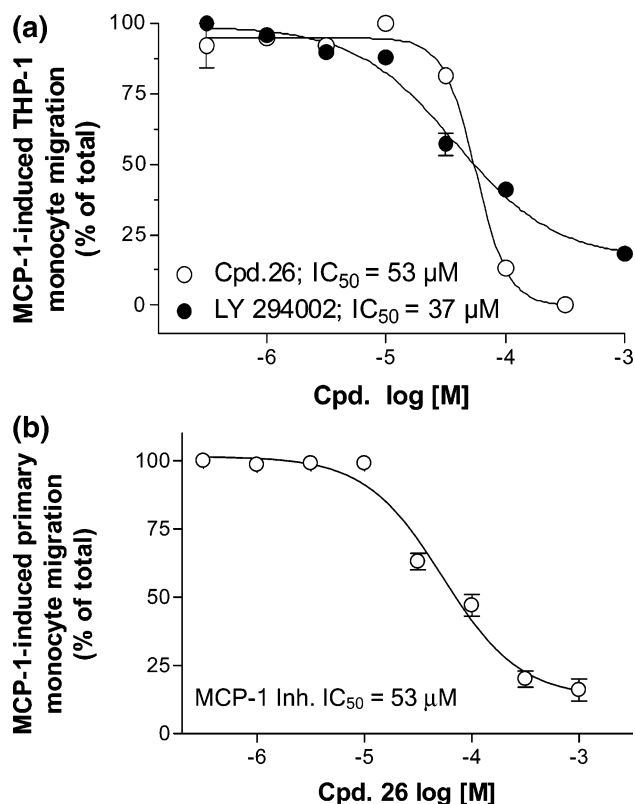

Figure 9. Blockade of MCP-1-induced monocyte chemotaxis. Graphs show inhibition curve of **26** in comparison with LY294002. After starvation of THP-1 (a) or primary bone marrow derived monocytes (b) and pretreatment with inhibitor or DMSO, as indicated, chemotaxis was induced with MCP-1 (10^{-9} M) as described in the section Biological Methods.

Table 9. Pharmacokinetic Parameters of **26** after Single Dose of 10 mg/kg in Rats

route	CL (L kg^{-1} h^{-1})	AUC (h ng mL^{-1})	C_{max} (ng mL^{-1})	$t_{1/2}$ (h)	V_d (L/kg)
iv	2.27	4401	11399	0.65	25.3
po		847	309	1	

followed by monocytes/macrophages and lymphocytes, recruitment of neutrophils was monitored 4 h after thioglycollate injection.[50]

Oral administration of **26** at 10 mg/kg resulted in moderate reduction of neutrophil recruitment (35% $\pm$ 14%), almost matching the result observed in PI3Kγ-deficient mice.[10] Given the short oral half-life of **26** ($t_{1/2}$ = 1 h) and relative high clearance (2.25 L kg^{-1} h^{-1}), investigations at later time points (24–48 h) to assess macrophage and monoycte recruitment were not undertaken (see Table 9). The modest pharmacokinetic properties did not appear to be caused by rapid oxidative metabolism (microsomal metabolism after 1 h: 16% (rat), 10% (human)). We suspect that the phenolic hydroxy group might be subject to glucoronidation and hence that compound **26** might be cleared via nonoxidative metabolism. Current efforts are focusing on generating analogues (including prodrugs) with more suitable pharmacokinetic profiles.

Conclusions

We have designed a new chemical series of potent PI3Kγ inhibitors. Through the use of X-ray crystallography and iterative docking experiments, the key molecular features of this series necessary for inhibitory activity against PI3Kγ have been identified to be the NH group of the thiazolidinedione core and the 2-hydroxy group on the phenyl ring. Introduction of an additional 4-fluoro substituent generated a key compound (**26**) with increased selectivity ratio between PI3Kγ and the class IA PI3K isoforms (α, β, δ). Notably, the isoform selectivity determined for compound **26** at the enzymatic level could subsequently be reproduced in cellular assays, where we show, for the first time, a compound inhibiting PI3Kγ (but not PI3Kα, PI3Kβ, and PI3Kδ) dependent pathways inside cells. Compound **26**, when tested in a murine peritonitis model, produced a similar decrease in leukocyte infiltration as previously observed with PI3Kγ-deficient mice.

General Experimental Methods

Procedures. All chemicals were purchased from Fluka-Aldrich, Buchs (CH), unless otherwise stated. Melting points were measured with a Büchi melting point apparatus B-545 and are not corrected. NMR spectra were recorded on a Bruker DPX 300 MHz spectrometer. Data were reported as follows: chemical shift δ in ppm using either residual DMSO (2.49 ppm) or CHCl$_3$ (7.19 ppm) as internal standards, multiplicity (s = singlet, d = doublet, t = triplet, q = quadruplet, m = multiplet), integration, and coupling constants (J) in hertz. MS data were obtained using a Perkin-Elmer API 150 EX (APCI) mass spectrometer. The analytical HPLC was performed using an HPLC Waters Symmetry C8 50 mm × 4.6 mm column with the following conditions: MeCN/H$_2$O, 0.09% TFA, 0% to 100% (8 min), max plot 230–400 nm. Elemental analyses were performed on an Erba Science 11108 CHN analyzer.

General Procedures for the Suzuki Reaction. Procedure A. The bromo derivative (100 mg, 1 equiv) was dissolved in a mixture (7/3) of dry toluene and ethanol (10 mL) and purged with inert argon gas for 10 min. Tetrakis(triphenylphosphine)palladium(0) (0.05 equiv) was then added followed by the corresponding boronic acid (1.1 equiv) and a 2 M aqueous potassium carbonate solution (3 equiv). The reaction mixture was refluxed for 12 h, then allowed to cool to room temperature The organic solvents were removed

manner with an IC$_{50}$ value of 52 μM, as well as in the monocytic cell line THP-1 with an IC$_{50}$ value of 53 μM (Figure 9).

In Vivo Pharmacology. To evaluate the efficacy of **26** to block leukocyte migration in vivo, it was tested in a mouse model of thioglycollate-induced peritonitis. Since neutrophils are the predominant cell type in the initial influx of leukocytes,

under vacuum, and the residue was taken up in ethyl acetate and washed with water and brine. The organic phases were finally dried over magnesium sulfate and evaporated to dryness to give a crude compound that was purified through a silica gel pad using dichloromethane as the eluent. The crude compounds were analyzed by LC/MS and used in the next step without further purification.

Procedure B. The corresponding bromo derivative (100 mg, 1 equiv), boronic acid (1.1 equiv), palladium(II) acetate (0.1 equiv), and 2 M aqueous potassium carbonate (3 equiv) were stirred in water (5 mL) at room temperature for 12 h under a nitrogen atmosphere. The reaction mixture was then neutralized by adding citric acid (10%) and extracted with ethyl acetate. The organic phase was washed with water and brine and dried over magnesium sulfate. It was then concentrated under vacuum to give the corresponding crude compound that was purified through a silica gel pad with dichloromethane as the eluent. The desired crude compound was analyzed by LC/MS and used in the next step without further purification.

General Procedure for the Knoevenagel Reaction. The corresponding aldehyde (1 equiv), β-alanine (2 equiv), and 2,4-thiazolidinedione (2 equiv) were heated at 100 °C for 1 h in glacial acetic acid (2 mL). Upon completion of the reaction, the mixture was cooled, the reaction was quenched with water, and the precipitate was filtered off. The solid was washed with water and methanol and then finally dried with diethyl ether to give the desired compound in high purity (>90%).

Preparation of 5-[5-(4-Fluoro-2-hydroxyphenyl)furan-2-yl-methylene]thiazolidine-2,4-dione (26) According to Scheme 2. 2-Benzyloxy-1-bromo-4-fluorobenzene (26c). 2-Bromo-5-fluorophenol (1.16 mL, 10.47 mmol, 1 equiv) was dissolved in THF (25 mL) in the presence of potassium carbonate (2.90 g, 20.94 mmol, 2 equiv). The reaction mixture was stirred at room temperature for 10 min. Benzyl bromide (1.50 mL, 12.57 mmol, 1.2 equiv) was added, and the reaction mixture was heated at 60 °C for 12 h before the reaction was quenched with water (20 mL). Ethyl acetate was added, the desired compound was extracted, and organic phases were washed several times with an aqueous potassium carbonate solution. The organic layer was dried over magnesium sulfate, evaporated under vacuum, and purified by flash chromatography using cyclohexane as eluent. An amount of 2 g of the expected compound (68%) was recovered as a white oil (HPLC: 95%, t_R = 4.51 min). ^{1}H NMR (CDCl$_3$, 300 MHz) δ 7.52–7.36 (m, 6H), 6.74–6.59 (m, 2H), 5.16 (m, 2H). MS (ES), m/z: 282.1 [M + H]$^+$.

5-(2-Benzyloxy-4-fluorophenyl)furan-2-carbaldehyde (26b). Compound **26c** (1.5 g, 5.34 mmol, 1 equiv) was dissolved in a mixture (7/3) of dry toluene and ethanol (25 mL) and purged with argon gas for 10 min. Tetrakis(triphenylphosphine)palladium(0) (590 mg, 0.53 mmol, 0.1 equiv) was then added followed by 5-formyl-2-furanboronic acid (821 mg, 5.87 mmol, 1.1 equiv) and a 2 M aqueous potassium carbonate solution (3 mL, 6 mmol). The reaction mixture was refluxed for 4 h before being cooled. The organic solvents were evaporated under vacuum, and the residue was redissolved in ethyl acetate, washed with water and brine, and finally dried over magnesium sulfate. Ethyl acetate was evaporated under vacuum to give a crude compound that was purified on a silica gel using cyclohexane/ethyl acetate (9/1) as eluent to give 880 mg of the expected compound (56%) as a white oil (HPLC: 94%, t_R = 4.30 min). ^{1}H NMR (CDCl$_3$, 300 MHz) δ 9.54 (s, 1H), 8.0–7.95 (m, 1H), 7.39–7.37 (m, 5H), 7.17 (d, 1H, J = 3 Hz), 6.91 (d, 1H, J = 3 Hz), 6.78–6.70 (m, 2H). MS (ES), m/z: 297.3 [M + H]$^+$, 295.3 [M − H]$^-$.

5-(4-Fluoro-2-hydroxyphenyl)furan-2-carbaldehyde (26a). Compound **26b** (650 mg, 2.19 mmol, 1 equiv) was dissolved in DCM (25 mL) under an inert atmosphere and cooled to −70 °C. Boron trichloride (1 M) (5.3 mL, 5.3 mmol, 2.4 equiv) was added slowly, and the reaction mixture was left at −70 °C for 30 min before the reaction was quenched slowly with water. The aqueous phase was made neutral to pH 7 by addition of a saturated potassium carbonate solution. The organic phase was decanted, dried over magnesium sulfate, and evaporated to give 300 mg (66%) of a yellow oil

(HPLC: 98%, t_R = 2.77 min). ^{1}H NMR (CDCl$_3$, 300 MHz) δ 9.80 (m, 1H), 9.50 (s, 1H), 7.70–7.60 (m, 1H), 7.15 (d, 1H, J = 3 Hz), 6.85 (d, 1H, J = 3 Hz), 6.50–6.35 (m, 2H). MS (ES), m/z: 207.2 [M + H]$^+$, 205.3 [M − H]$^-$. The intermediate aldehyde **26a** can also be synthesized in one step according to procedure A in 4% yield.

5-[5-(4-Fluoro-2-hydroxyphenyl)furan-2-ylmethylene]thiazolidine-2,4-dione (26). Compound **26a** (175 mg, 0.85 mmol, 1 equiv), β-alanine (151 mg, 1.7 mmol, 2 equiv), and 2,4-thiazolidinedione (200 mg, 1.7 mmol, 2 equiv) were heated at 100 °C for 1 h in acetic acid (3 mL). Water (0.5 mL) was added, and the resulting precipitate was filtered off to give 245 mg (95%) of the expected compound as a yellow solid. Treatment with 2 equiv of KOH (1 M) gave the desired bis-potassium salt as a red powder (HPLC: 96.20%, t_R = 3.44 min), mp >400 °C. ^{1}H NMR (DMSO-d_6) δ 7.38 (d, 1H, J = 9 Hz), 7.28 (d, 1H, J = 3 Hz), 7.02 (s, 1H), 6.58 (d, 1H, J = 3 Hz), 5.78–5.73 (m, 2H). MS (ES), m/z: 304.09 [M − H]$^-$. Anal. (C$_{14}$H$_6$FK$_2$NO$_4$S) C, H, N.

5-[5-Phenyl)furan-2-ylmethylene]thiazolidine-2, 4-dione (1). Aldehyde **1a** is commercially available from Aldrich. The Knoevenagel reaction was performed starting from 100 mg of **1a**. The title compound (150 mg) was obtained in 95% yield following the general procedure for the Knoevenagel reaction (HPLC: 99.9%, t_R = 3.74 min), mp 262–264 °C. ^{1}H NMR (DMSO-d_6) δ 12.48 (m, 1H), 7.82 (m, 2H), 7.65 (s, 1H), 7.53 (m, 2H), 7.41 (m, 1H), 7.28 (d, 1H, J = 3 Hz), 7.24 (d, 1H, J = 3 Hz). MS (ES), m/z: 272.8 [M + H]$^+$, 270.16 [M − H]$^-$. Anal. (C$_{14}$H$_9$NO$_3$S) C, H, N.

5-[5-(2-Hydroxyphenyl)furan-2-ylmethylene]thiazolidine-2, 4-dione (2). Intermediate aldehyde **2a** (11 mg) was synthesized according to procedure A in 10% yield. MS (ES), m/z: 187.2 [M − H]$^-$. The title compound (6 mg) was obtained in 35% yield following the general procedure for the Knoevenagel reaction (HPLC: 91.97%, t_R = 3.45 min), mp 290–292 °C. ^{1}H NMR (DMSO-d_6) δ 12.50 (m, 1H), 9.80 (m, 1H), 7.70 (m, 1H), 7.60 (m, 2H), 7.50 (s, 1H), 6.80 (m, 2H), 6.60 (d, 1H, J = 3 Hz). MS (ES), m/z: 288.1 [M + H]$^+$, 286.10 [M − H]$^-$. Anal. (C$_{14}$H$_9$NO$_4$S) C, H, N.

5-[5-(3-Hydroxyphenyl)furan-2-ylmethylene]thiazolidine-2,4-dione (3). Intermediate aldehyde **3a** (15 mg) was synthesized according to procedure A in 14% yield. MS (ES), m/z: 187.2 [M − H]$^-$. The title compound (5 mg) was obtained in 22% yield following the general procedure for the Knoevenagel reaction (HPLC: 90.4%, t_R = 3.32 min), mp 280–281 °C. ^{1}H NMR (DMSO-d_6) δ 12.45 (m, 1H), 9.80 (m, 1H), 7.63 (s, 1H), 7.31–7.20 (m, 5H), 6.80 (d, 1H, J = 3 Hz). MS (ES), m/z: 288.7 [M + H]$^+$, 286.7 [M − H]$^-$. Anal. (C$_{14}$H$_9$NO$_4$S) C, H, N.

5-[5-(4-Hydroxyphenyl)furan-2-ylmethylene]thiazolidine-2, 4-dione (4). Intermediate aldehyde **4a** (11 mg) was synthesized according to procedure A in 10% yield. MS (ES), m/z: 187.2 [M − H]$^-$. The title compound (12 mg) was obtained in 68% yield following the general procedure for the Knoevenagel reaction (HPLC: 96.5%, t_R = 3.62 min), mp 269–270 °C. ^{1}H NMR (DMSO-d_6) δ 12.55 (m, 1H), 9.80 (m, 1H), 7.65 (d, 2H, J = 9 Hz), 7.60 (s, 1H), 7.19 (d, 1H, J = 3 Hz), 7.05 (d, 1H, J = 3 Hz), 6.90 (d, 2H, J = 9 Hz). MS (ES), m/z: 288.1 [M + H]$^+$, 286.10 [M − H]$^-$. Anal. (C$_{14}$H$_9$NO$_4$S) C, H, N.

5-[5-(2-Methoxyphenyl)furan-2-ylmethylene]thiazolidine-2,4-dione (5). Intermediate aldehyde **5a** (20 mg) was synthesized according to procedure A in 18% yield. MS (ES), m/z: 201.2 [M − H]$^-$. The title compound (12 mg) was obtained in 41% yield following the general procedure for the Knoevenagel reaction (HPLC: 93.25%, t_R = 3.74 min), mp 270–272 °C. ^{1}H NMR (DMSO-d_6) δ 12.50 (m, 1H), 7.81 (d, 1H, J = 3 Hz), 7.64 (s, 1H), 7.43–7.38 (m, 1H), 7.23–7.14 (m, 4H), 3.95 (s, 3H). MS (ES), m/z: 302.3 [M + H]$^+$, m/z: 300.3 [M − H]$^-$. Anal. (C$_{15}$H$_{11}$NO$_4$S) C, H, N.

5-[5-(2-Chlorophenyl)furan-2-ylmethylene]thiazolidine-2,4-dione (6). Aldehyde **6a** is commercially available from Aldrich. The Knoevenagel reaction was performed starting from 100 mg of **6a**. The title compound (134 mg) was obtained in 90% yield following the general procedure for the Knoevenagel reaction (HPLC: 99.3%,

t_R = 4.08 min), mp 268−270 °C. ^{1}H NMR (DMSO-d_6) δ 12.53 (m, 1H), 7.92 (dd, 1H, J = 9, 3 Hz), 7.68 (s, 1H), 7.70−7.55 (m, 2H), 7.47 (m, 1H), 7.42 (d, 1H, J = 3 Hz), 7.27 (d, 1H, J = 3 Hz). MS (ES), m/z: 306.10 [M + H]$^+$, 304.10 [M − H]$^-$. Anal. (C$_{14}$H$_8$ClNO$_3$S) C, H, N.

5-[5-(2-Fluorophenyl)furan-2-ylmethylene]thiazolidine-2,4-dione (7). Intermediate aldehyde **7a** (53 mg) was synthesized according to procedure A in 50% yield. MS (ES), m/z: 191.2 [M + H]$^+$. The title compound (55 mg) was obtained in 69% yield following the general procedure for the Knoevenagel reaction (HPLC: 96.2%, t_R = 4.09 min), mp 240−242 °C. ^{1}H NMR (DMSO-d_6) δ 12.53 (m, 1H), 7.88 (m, 1H), 7.84 (s, 1H), 7.45 (m, 3H), 7.26 (d, 1H, J = 3 Hz), 7.12 (d, 1H, J = 3 Hz). MS (ES), m/z: 288.2 [M − H]$^-$. Anal. (C$_{14}$H$_8$FNO$_3$S) C, H, N.

2-[5-(2,4-Dioxothiazolidin-5-ylidenemethyl)furan-2-yl]benzoic Acid (8). Intermediate aldehyde **8a** (30 mg) was synthesized according to procedure A in 27% yield. MS (ES), m/z: 215.2 [M − H]$^-$. The title compound (14 mg) was obtained in 32% yield following the general procedure for the Knoevenagel reaction (HPLC: 94.6%, t_R = 2.20 min), mp 220−222 °C. ^{1}H NMR (DMSO-d_6) δ 13.20 (m, 1H), 12.46 (m, 1H), 7.75 (m, 2H), 7.65 (m, 1H), 7.63 (s, 1H), 7.53 (m,1H), 7.22 (d, 1H, J = 3 Hz), 7.01 (d, 1H, J = 3 Hz). MS (ES), m/z: 314.3 [M − H]$^-$. Anal. (C$_{15}$H$_9$NO$_5$S) C, H, N.

2-[5-(2,4-Dioxothiazolidin-5-ylidenemethyl)furan-2-yl]benzoic Acid Methyl Ester (9). Intermediate aldehyde **9a** (12 mg) was synthesized according to procedure A in 10% yield. MS (ES), m/z: 231.2 [M + H]$^+$. The title compound (6 mg) was obtained in 36% yield following the general procedure for the Knoevenagel reaction (HPLC: 93.0%, t_R = 3.24 min), mp 190−192 °C. ^{1}H NMR (DMSO-d_6) δ 12.48 (m, 1H), 7.75−7.70 (m, 3H), 7.62 (s, 1H), 7.56 (m,1H), 7.22 (d, 1H, J = 3 Hz), 7.02 (d, 1H, J = 3 Hz), 3.79 (s, 3H). MS (ES), m/z: 330.3 [M + H]$^+$, 328.3 [M − H]$^-$. Anal. (C$_{16}$H$_{11}$NO$_5$S) C, H, N.

2-[5-(2,4-Dioxothiazolidin-5-ylidenemethyl)furan-2-yl]phenylacetic Acid (10). Intermediate aldehyde **10a** (43 mg) was synthesized according to procedure A in 41% yield. MS (ES), m/z: 229.2 [M − H]$^-$. The title compound (15 mg) was obtained in 25% yield following the general procedure for the Knoevenagel reaction (HPLC: 97.4%, t_R = 2.70 min), mp 232−234 °C. ^{1}H NMR (DMSO-d_6) δ 12.50 (m, 2H), 7.76 (d, 1H, J = 9 Hz), 7.64 (s, 1H), 7.47−7.41 (m, 3H), 7.24 (d, 1H, J = 3 Hz), 6.99 (d, 1H, J = 3 Hz), 3.91 (s, 2H). MS (ES), m/z: 328.3 [M − H]$^-$. Anal. (C$_{16}$H$_{11}$NO$_5$S) C, H, N.

3-[5-(2,4-Dioxothiazolidin-5-ylidenemethyl)furan-2-yl]benzoic Acid (11). Intermediate aldehyde **11a** (48 mg) was synthesized according to procedure A in 45% yield. MS (ES), m/z: 215.2 [M − H]$^-$. The title compound (31 mg) was obtained in 45% yield following the general procedure for the Knoevenagel reaction (HPLC: 94%, t_R = 2.15 min), mp 358−360 °C. ^{1}H NMR (DMSO-d_6) δ 13.15 (m, 1H), 12.51 (m, 1H), 8.36 (m, 1H), 8.05 (m, 1H), 7.94 (m, 1H), 7.66 (m, 2H), 7.41 (d, 1H, J = 3 Hz), 7.24 (d, 1H, J = 3 Hz). MS (ES), m/z: 314.3 [M − H]$^-$. Anal. (C$_{15}$H$_9$NO$_5$S) C, H, N.

3-[5-(2,4-Dioxothiazolidin-5-ylidenemethyl)furan-2-yl]benzoic Acid Methyl Ester (12). Intermediate aldehyde **12a** (12 mg) was synthesized according to procedure A in 10% yield. MS (ES), m/z: 231.2 [M + H]$^+$. The title compound (5 mg) was obtained in 26% yield following the general procedure for the Knoevenagel reaction (HPLC: 92.0%, t_R = 3.31 min), mp 320−322 °C. ^{1}H NMR (DMSO-d_6) δ 12.50 (m, 1H), 8.33 (m, 1H), 8.03 (dd, 1H, J = 9, 3 Hz), 7.88 (d, 1H, J = 9 Hz), 7.64 (m, 1H), 7.26 (d, 1H, J = 3 Hz), 7.15 (s, 1H), 6.80 (d, 1H, J = 3 Hz), 3.91 (s, 3H). MS (ES), m/z: 330.3 [M + H]$^+$, 328.3 [M − H]$^-$. Anal. (C$_{16}$H$_{11}$NO$_5$S) C, H, N.

3-[5-(2,4-Dioxothiazolidin-5-ylidenemethyl)furan-2-yl]phenyl Acetic Acid (13). Intermediate aldehyde **13a** (33 mg) was synthesized according to procedure A in 30% yield. MS (ES), m/z: 229.2 [M − H]$^-$. The title compound (17 mg) was obtained in 36% yield following the general procedure for the Knoevenagel reaction (HPLC: 94.3%, t_R = 2.72 min), mp 210−212 °C. ^{1}H NMR

(DMSO-d_6) δ 12.60 (m, 2H), 7.72 (m, 2H), 7.64 (s, 1H), 7.47 (m, 1H), 7.31 (d, 1H, J = 3 Hz), 7.27 (d, 1H, J = 3 Hz), 7.26 (d, 1H, J = 3 Hz), 3.67 (s, 2H). MS (ES), m/z: 328.3 [M − H]$^-$. Anal. (C$_{16}$H$_{11}$NO$_5$S) C, H, N.

N-[2-(5-(2,4-Dioxothiazolidin-5-ylidenemethyl)furan-2-yl)phenyl]acetamide (14). Intermediate aldehyde **14a** (72 mg) was synthesized according to procedure A in 68% yield. MS (ES), m/z: 230.2 [M + H]$^+$. The title compound (49 mg) was obtained in 48% yield following the general procedure for the Knoevenagel reaction (HPLC: 93.5%, t_R = 3.65 min), mp 251−253 °C. ^{1}H NMR (DMSO-d_6) δ 12.50 (m, 1H), 9.71 (m, 1H), 7.78 (m, 1H), 7.76 (s, 1H), 7.46−7.40 (m, 3H), 7.24 (d, 1H, J = 3 Hz), 7.03 (d, 1H, J = 3 Hz), 2.08 (s, 3H). MS (ES), m/z: 329.3 [M + H]$^+$, 327.3 [M − H]$^-$. Anal. (C$_{16}$H$_{12}$N$_2$O$_4$S) C, H, N.

5-[5-(2-Amino-5-nitrophenyl)furan-2-ylmethylene]thiazolidine-2,4-dione (15). Intermediate aldehyde **15a** (11 mg) was synthesized according to procedure A in 10% yield. MS (ES), m/z: 233.2 [M + H]$^+$. The title compound (1.5 mg) was obtained in 10% yield following the general procedure for the Knoevenagel reaction (HPLC: 95.5%, t_R = 2.51 min). MS (ES), m/z: 332.3 [M + H]$^+$, 330.3 [M − H]$^-$.

5-[5-(2-Hydroxyphenyl)thiophen-2-ylmethylene]thiazolidine-2,4-dione (16). Intermediate aldehyde **16a** (13 mg) was synthesized according to procedure A in 10% yield. MS (ES), m/z: 203.2 [M − H]$^-$. The title compound (8 mg) was obtained in 40% yield following the general procedure for the Knoevenagel reaction (HPLC: 98%, t_R = 3.29 min), mp 270−272 °C. ^{1}H NMR (DMSO-d_6) δ 12.51 (m, 1H), 10.69 (m, 1H), 8.03 (s, 1H), 7.79−7.75 (m, 2H), 7.64 (d, 1H, J = 3 Hz), 7.24−7.18 (m, 1H), 6.97−6.90 (m, 2H). MS (ES), m/z: 304.2 [M + H]$^+$, 302.2 [M − H]$^-$. Anal. (C$_{14}$H$_9$NO$_3$S$_2$) C, H, N.

5-[5-(3-Methoxyphenyl)furan-2-ylmethylene]thiazolidine-2,4-dione (17). Intermediate aldehyde **17a** (21 mg) was synthesized according to procedure A in 19% yield. MS (ES), m/z: 201.2 [M − H]$^-$. The title compound (17 mg) was obtained in 55% yield following the general procedure for the Knoevenagel reaction (HPLC: 99.78%, t_R = 3.90 min), mp 240−243 °C. ^{1}H NMR (DMSO-d_6) δ 12.50 (m, 1H), 7.65 (s, 1H), 7.46−7.35 (m, 4H), 7.23 (d, 1H, J = 3 Hz), 7.05 (d, 1H, J = 3 Hz), 3.84 (s, 3H). MS (ES), m/z: 302.2 [M + H]$^+$, 300.2 [M − H]$^-$. Anal. (C$_{15}$H$_{11}$NO$_4$S) C, H, N.

5-[5-(3-Nitrophenyl)furan-2-ylmethylene]thiazolidine-2,4-dione (18). Intermediate aldehyde **18a** (20 mg) was synthesized according to procedure A in 20% yield. MS (ES), m/z: 218.2 [M + H]$^+$. The title compound (22 mg) was obtained in 75% yield following the general procedure for the Knoevenagel reaction (HPLC: 98.17%, t_R = 3.85 min), mp 230−232 °C. ^{1}H NMR (DMSO-d_6) δ 12.54 (m, 1H), 8.57 (m, 1H), 8.22 (m, 2H), 7.82 (m, 1H), 7.67 (s, 1H), 7.56 (d, 1H, J = 3 Hz), 7.28 (d, 1H, J = 3 Hz). MS (ES), m/z: 315.3 [M − H]$^-$. Anal. (C$_{14}$H$_8$N$_2$O$_5$S) C, H, N.

5-(5-Benzo[1,3]dioxol-5-yl-furan-2-ylmethylene)thiazolidine-2,4-dione (19). Intermediate aldehyde **19a** (11 mg) was synthesized according to procedure A in 10% yield. MS (ES), m/z: 217.2 [M + H]$^+$. The title compound (5 mg) was obtained in 34% yield following the general procedure for the Knoevenagel reaction (HPLC: 98.9%, t_R = 4.40min), mp 295−298 °C. ^{1}H NMR (DMSO-d_6) δ 12.45 (m, 1H), 7.61 (s, 1H), 7.37 (m, 2H), 7.20 (d, 1H, J = 3 Hz), 7.16 (d, 1H, J = 3 Hz), 7.10 (d, 1H, J = 9 Hz), 6.11 (s, 2H). MS (ES), m/z: 316.1 [M + H]$^+$, 314.3 [M − H]$^-$. Anal. (C$_{15}$H$_9$NO$_5$S) C, H, N.

5-[2,3′]Bifuranyl-5-ylmethylenethiazolidine-2,4-dione (20). Intermediate aldehyde **20a** (43 mg) was synthesized according to procedure B in 40% yield. MS (ES), m/z: 163.2 [M + H]$^+$. The title compound (38 mg) was obtained in 55% yield following the general procedure for the Knoevenagel reaction (HPLC: 96.2%, t_R = 4.53 min), mp 255−257 °C. ^{1}H NMR (DMSO-d_6) δ 12.43 (m, 1H), 8.22 (m, 1H), 7.83 (m, 1H), 7.60 (s, 1H), 7.18 (d, 1H, J = 3 Hz), 6.95 (d, 1H, J = 3 Hz), 6.91 (m, 1H). MS (ES), m/z: 262.2 [M + H]$^+$, 260.2 [M − H]$^-$. Anal. (C$_{12}$H$_7$NO$_4$S) C, H, N.

5-(5′-Nitro[2,2′]bifuranyl-5-ylmethylene)thiazolidine-2,4-dione (21). Intermediate aldehyde **21a** (42 mg) was synthesized

according to procedure B in 40% yield. MS (ES), *m/z*: 208.1 [M + H]⁺. The title compound (34 mg) was obtained in 55% yield following the general procedure for the Knoevenagel reaction (HPLC: 95.4%, t_R = 4.83 min), mp 328−330 °C. ¹H NMR (DMSO-d_6) δ 12.59 (m, 1H), 7.87 (d, 1H, *J* = 3 Hz), 7.67 (s, 1H), 7.41 (d, 1H, *J* = 3 Hz), 7.28 (m, 2H). MS (ES), *m/z*: 307.2 [M + H]⁺. Anal. (C₁₂H₆N₂O₆S) C, H, N.

5-(5-Pyridin-2-ylfuran-2-ylmethylene)thiazolidine-2,4-dione (22). Intermediate aldehyde **22a** (25 mg) was synthesized according to procedure A in 23% yield. MS (ES), *m/z*: 174.1 [M + H]⁺. The title compound (20 mg) was obtained in 52% yield following the general procedure for the Knoevenagel reaction (HPLC: 96.77%, t_R = 3.69 min), mp 225−227 °C. ¹H NMR (DMSO-d_6) δ 12.50 (m, 1H), 8.70 (dd, 1H, *J* = 6, 3 Hz), 8.10 (m, 1H), 7.90 (m, 1H), 7.65 (m, 1H), 7.27 (d, 1H, *J* = 3 Hz), 7.10 (s, 1H), 6.80 (d, 1H, *J* = 3 Hz). MS (ES), *m/z*: 273.2 [M + H]⁺, 271.2 [M − H]⁻. Anal. (C₁₃H₈N₂O₃S) C, H, N.

5-(5-Pyridin-3-ylfuran-2-ylmethylene)thiazolidine-2,4-dione (23). Intermediate aldehyde **23a** (32 mg) was synthesized according to procedure A in 30% yield. MS (ES), *m/z*: 174.1 [M + H]⁺. The title compound (20 mg) was obtained in 40% yield following the general procedure for the Knoevenagel reaction (HPLC: 93.7%, t_R = 3.80 min), mp 332−335 °C. ¹H NMR (DMSO-d_6) δ 12.52 (m, 1H), 9.05 (d, 1H, *J* = 3 Hz), 8.58 (dd, 1H, *J* = 6, 3 Hz), 8.16 (m, 1H), 7.67 (s, 1H), 7.56 (m, 1H), 7.44 (d, 1H, *J* = 3 Hz), 7.26 (d, 1H, *J* = 3 Hz). MS (ES), *m/z*: 273.2 [M + H]⁺, 271.2 [M − H]⁻. Anal. (C₁₃H₈N₂O₃S) C, H, N.

5-(5-Quinolin-2-ylfuran-2-ylmethylene)thiazolidine-2,4-dione (24). Intermediate aldehyde **24a** (14 mg) was synthesized according to procedure A in 13% yield. MS (ES), *m/z*: 224.2 [M + H]⁺. The title compound (6 mg) was obtained in 33% yield following the general procedure for the Knoevenagel reaction (HPLC: 98%, t_R = 3.15 min), mp 302−305 °C. ¹H NMR (DMSO-d_6) δ 12.56 (m, 1H), 8.55 (d, 1H, *J* = 9 Hz), 8.05−7.98 (m, 3H), 7.80 (m, 1H), 7.72 (s, 1H), 7.63 (m, 1H), 7.55 (d, 1H, *J* = 3 Hz), 7.31 (d, 1H, *J* = 3 Hz). MS (ES), *m/z*: 323.2 [M + H]⁺, 321.2 [M − H]⁻. Anal. (C₁₇H₁₀N₂O₃S) C, H, N.

5-(5-Quinolin-8-ylfuran-2-ylmethylene)thiazolidine-2,4-dione (25). Intermediate aldehyde **25a** (12 mg) was synthesized according to procedure A in 11% yield. MS (ES), *m/z*: 224.2 [M + H]⁺. The title compound (5 mg) was obtained in 26% yield following the general procedure for the Knoevenagel reaction (HPLC: 99%, t_R = 3.28 min), mp 295−297 °C. ¹H NMR (DMSO-d_6) δ 12.50 (m, 1H), 9.05 (dd, 1H, *J* = 6, 3 Hz), 8.48 (dd, 1H, *J* = 9, 3 Hz), 8.27 (dd, 1H, *J* = 9, 1 Hz), 8.08 (d, 1H, *J* = 6 Hz,), 8.05 (m, 1H), 7.83 (m, 1H), 7.71 (s, 1H), 7.65 (dd, 1H, *J* = 9, 6 Hz), 7.31 (d, 1H, *J* = 6 Hz). MS (ES), *m/z*: 323.2 [M + H]⁺, 321.2 [M − H]⁻. Anal. (C₁₇H₁₀N₂O₃S) C, H, N.

5-[5-(2,4-Dihydroxyphenyl)furan-2-ylmethylene]thiazolidine-2,4-dione (27). Intermediate aldehyde **27a** (34 mg) was synthesized according to procedure B in 32% yield. MS (ES), *m/z*: 205.2 [M + H]⁺. The title compound (26 mg) was obtained in 52% yield following the general procedure for the Knoevenagel reaction (HPLC: 95.2%, t_R = 3.05 min), mp 296−300 °C. ¹H NMR (DMSO-d_6) δ 12.36 (m, 1H), 10.36 (m, 1H), 9.82 (m, 1H), 7.60 (s, 1H), 7.55 (d, 1H, *J* = 9 Hz), 7.18 (d, 1H, *J* = 3 Hz), 6.98 (d, 1H, *J* = 3 Hz), 6.46 (m, 2H). MS (ES), *m/z*: 304.3 [M + H]⁺, 302.3 [M − H]⁻. Anal. (C₁₄H₉NO₅S) C, H, N.

4-[5-(2,4-Dioxothiazolidin-5-ylidenemethyl)furan-2-yl]-3-hydroxybenzoic Acid Methyl Ester (28). Intermediate aldehyde **28a** (11 mg) was synthesized according to procedure B in 10% yield. MS (ES), *m/z*: 245.2 [M − H]⁻. The title compound (10 mg) was obtained in 62% yield following the general procedure for the Knoevenagel reaction (HPLC: 98.5%, t_R = 3.22 min), mp 340−345 °C. ¹H NMR (DMSO-d_6) δ 12.49 (m, 1H), 10.94 (m, 1H), 7.82 (d, 1H, *J* = 9 Hz), 7.66 (s, 1H), 7.60 (m, 2H), 7.33 (d, 1H, *J* = 3 Hz), 7.24 (d, 1H, *J* = 3 Hz), 3.85 (s, 3H). MS (ES), *m/z*: 346.3 [M + H]⁺, 344.3 [M − H]⁻. Anal. (C₁₆H₁₁NO₆S) C, H, N.

5-[5-(5-Fluoro-2-hydroxyphenyl)furan-2-ylmethylene]thiazolidine-2,4-dione (29). Intermediate aldehyde **29a** (21 mg) was synthesized according to procedure B in 20% yield. MS (ES), *m/z*:

207.1 [M + H]⁺. The title compound (2 mg) was obtained in 5% yield following the general procedure for the Knoevenagel reaction (HPLC: 98.2%, t_R = 3.51 min). MS (ES), *m/z*: 306.4 [M + H]⁺, 304.4 [M − H]⁻.

5-[5-(2-Hydroxy-5-chlorophenyl)furan-2-ylmethylene]thiazolidine-2,4-dione (30). Intermediate aldehyde **30a** (42 mg) was synthesized according to procedure B in 40% yield. MS (ES), *m/z*: 221.5 [M − H]⁻. The title compound (27 mg) was obtained in 45% yield following the general procedure for the Knoevenagel reaction (HPLC: 97.2%, t_R = 4.10min), mp 320−322 °C. ¹H NMR (DMSO-d_6) δ 12.50 (m, 1H), 10.84 (m, 1H), 7.66 (s, 1H), 7.63 (d, 1H, *J* = 3 Hz), 7.25 (m, 3H), 7.02 (d, 1H, *J* = 3 Hz). MS (ES), *m/z*: 322.5 [M + H]⁺, 320.5 [M − H]⁻. Anal. (C₁₄H₈ClNO₄S) C, H, N.

3-[5-(2,4-Dioxothiazolidin-5-ylidenemethyl)furan-2-yl]-4-hydroxybenzonitrile (31). Intermediate aldehyde **31a** (68 mg) was synthesized according to procedure B in 65% yield. MS (ES), *m/z*: 212.1 [M − H]⁻. The title compound (33 mg) was obtained in 33% yield following the general procedure for the Knoevenagel reaction (HPLC: 95.7%, t_R = 3.25 min), mp 317−320 °C. ¹H NMR (DMSO-d_6) δ 12.51 (m, 1H), 11.78 (m, 1H), 7.68 (m, 2H), 7.27 (m, 3H), 7.18 (m, 1H). MS (ES), *m/z*: 313.3 [M + H]⁺, 311.3 [M − H]⁻. Anal. (C₁₅H₈N₂O₄S) C, H, N.

5-[5-(2-Hydroxy-5-trifluoromethoxyphenyl)furan-2-ylmethylene]thiazolidine-2,4-dione (32). Intermediate aldehyde **32a** (20 mg) was synthesized according to procedure B in 18% yield. MS (ES), *m/z*: 271.2 [M − H]⁻. The title compound (20 mg) was obtained in 71% yield following the general procedure for the Knoevenagel reaction (HPLC: 95.9%, t_R = 3.58 min), mp 304−305 °C. ¹H NMR (DMSO-d_6) δ 12.50 (m, 1H), 10.97 (m, 1H), 7.67 (s, 1H), 7.59 (d, 1H, *J* = 3 Hz), 7.24 (m, 3H), 7.08 (d, 1H, *J* = 3 Hz). MS (ES), *m/z*: 372.3 [M + H]⁺, 370.3 [M − H]⁻. Anal. (C₁₅H₈F₃NO₅S) C, H, N.

5-[5-(2-Hydroxy-5-methylphenyl)furan-2-ylmethylene]thiazolidine-2,4-dione (33). Intermediate aldehyde **33a** (52 mg) was synthesized according to procedure B in 50% yield. MS (ES), *m/z*: 201.2 [M − H]⁻. The title compound (31 mg) was obtained in 40% yield following the general procedure for the Knoevenagel reaction (HPLC: 97.9%, t_R = 3.79 min), mp 275−277 °C. ¹H NMR (DMSO-d_6) δ 12.45 (m, 1H), 10.25 (m, 1H), 7.65 (s, 1H), 7.52 (d, 1H, *J* = 3 Hz), 7.22 (d, 1H, *J* = 3 Hz), 7.17 (d, 1H, *J* = 3 Hz), 7.05 (dd, 1H, *J* = 9, 3 Hz), 6.90 (d, 1H, *J* = 9 Hz), 2.30 (s, 3H). MS (ES), *m/z*: 302.3 [M + H]⁺, 300.3 [M − H]⁻. Anal. (C₁₅H₁₁NO₄S) C, H, N.

5-[5-(2,5-Dihydroxyphenyl)furan-2-ylmethylene]thiazolidine-2,4-dione (34). Intermediate aldehyde **34a** (36 mg) was synthesized according to procedure B in 34% yield. MS (ES), *m/z*: 205.2 [M + H]⁺. The title compound (10 mg) was obtained in 19% yield following the general procedure for the Knoevenagel reaction (HPLC: 94.7%, t_R = 2.95 min), mp 263−265 °C. ¹H NMR (DMSO-d_6) δ 12.42 (m, 1H), 9.78 (m, 1H), 9.17 (m, 1H), 7.63 (s, 1H), 7.20 (m, 3H), 6.81 (d, 1H, *J* = 3 Hz), 6.65 (d, 1H, *J* = 3 Hz). MS (ES), *m/z*: 304.3 [M + H]⁺, 302.3 [M − H]⁻. Anal. (C₁₄H₉NO₅S) C, H, N.

5-[5-(2-Hydroxy-3-nitrophenyl)furan-2-ylmethylene]thiazolidine-2,4-dione (35). Intermediate aldehyde **35a** (33 mg) was synthesized according to procedure B in 32% yield. MS (ES), *m/z*: 234.1 [M + H]⁺. The title compound (9 mg) was obtained in 20% yield following the general procedure for the Knoevenagel reaction (HPLC: 97.1%, t_R = 3.51 min). MS (ES), *m/z*: 333.3 [M + H]⁺, 331.3 [M − H]⁻.

3-[5-(2,4-Dioxothiazolidin-5-ylidenemethyl)furan-2-yl]-4-hydroxybenzoic Acid (36). Intermediate aldehyde **36a** (50 mg) was synthesized according to procedure B in 47% yield. MS (ES), *m/z*: 231.2 [M − H]⁻. The title compound (54 mg) was obtained in 75% yield following the general procedure for the Knoevenagel reaction (HPLC: 90.5%, t_R = 3.52 min), mp 310−311 °C. ¹H NMR (DMSO-d_6) δ 13.40 (m, 1H), 12.50 (m, 2H), 8.50 (m, 1H), 8.00 (m, 1H), 7.70 (s, 1H), 7.53 (m, 1H), 7.29 (d, 1H, *J* = 3 Hz), 7.20 (d, 1H, *J* = 3 Hz). MS (ES), *m/z*: 332.1 [M − H]⁻.

5-[5-(4-Fluoro-2-methoxyphenyl)furan-2-ylmethylene]thiazo-lidine-2,4-dione (37). Intermediate aldehyde **37a** (12 mg) was synthesized according to procedure A in 11% yield. MS (ES), *m/z*: 219.2 [M − H]⁻. The title compound (10 mg) was obtained in 55% yield following the general procedure for the Knoevenagel reaction (HPLC: 98.9%, t_R = 3.74 min), mp 263−265 °C. ¹H NMR (DMSO-d_6) δ 12.46 (m, 1H), 7.84 (m, 1H), 7.64 (s, 1H), 7.22 (d, 1H, *J* = 3 Hz), 7.10−7.15 (m, 2H), 7.05 (m, 1H), 3.97 (s, 3H). MS (ES), *m/z*: 320.3 [M + H]⁺, 318.3 [M − H]⁻. Anal. ($C_{15}H_{10}$-FNO_4S) C, H, N.

5-[5-(4-Fluoro-2-hydroxyphenyl)thiophen-2-ylmethylene]thi-azolidine-2,4-dione (38). Intermediate aldehyde **38a** (14 mg) was synthesized according to procedure A in 9% yield. MS (ES), *m/z*: 221.5 [M − H]⁻. The title compound (10 mg) was obtained in 45% yield following the general procedure for the Knoevenagel reaction (HPLC: 95.1%, t_R = 3.64 min), mp 250−251 °C. ¹H NMR (DMSO-d_6) δ 12.50 (m, 1H), 11.23 (m, 1H), 8.02 (s, 1H), 7.83 (m, 1H), 7.74 (d, 1H, *J* = 3 Hz), 7.64 (d, 1H, *J* = 3 Hz), 6.78−6.74 (m, 2H). MS (ES), *m/z*: 322.5 [M + H]⁺, 320.5 [M − H]⁻. Anal. ($C_{14}H_8FNO_3S_2$) C, H, N.

5-[5-(2-Fluoro-4-hydroxyphenyl)furan-2-ylmethylene]thiazo-lidine-2,4-dione (39). Intermediate aldehyde **39a** (15 mg) was synthesized according to procedure B in 13% yield. MS (ES), *m/z*: 205.2 [M − H]⁻. The title compound (5 mg) was obtained in 21% yield following the general procedure for the Knoevenagel reaction (HPLC: 94.9%, t_R = 3.46min), mp 298−300 °C. ¹H NMR (DMSO-d_6) δ 12.45 (m, 1H), 10.47 (m, 1H), 7.68 (m, 1H), 7.63 (s, 1H), 7.22 (d, 1H, *J* = 3 Hz), 6.91−6.83 (m, 2H), 6.77 (dd, 1H, *J* = 15, 3 Hz). MS (ES), *m/z*: 306.2 [M + H]⁺, 304.2 [M − H]⁻. Anal. ($C_{14}H_8FNO_4S$) C, H, N.

5-[5-(2,4-Difluorophenyl)furan-2-ylmethylene]thiazolidine-2,4-dione (40). Intermediate aldehyde **40a** (68 mg) was synthesized according to procedure A in 65% yield. MS (ES), *m/z*: 209.2 [M + H]⁺. The title compound (69 mg) was obtained in 69% yield following the general procedure for the Knoevenagel reaction (HPLC: 100%, t_R = 4.14 min), mp 287−290 °C. ¹H NMR (DMSO-d_6) δ 12.52 (m, 1H), 7.90 (m, 1H), 7.67 (s, 1H), 7.50 (m, 1H), 7.35 (dd, 1H, *J* = 9, 3 Hz), 7.26 (d, 1H, *J* = 3 Hz), 7.02 (d, 1H, *J* = 3 Hz). MS (ES), *m/z*: 306.2 [M − H]⁻. Anal. ($C_{14}H_7F_2NO_3S$) C, H, N.

5-[5-(3,5-Difluoro-2-hydroxyphenyl)furan-2-ylmethylene]thi-azolidine-2,4-dione (41). Intermediate aldehyde **41a** (7 mg) was synthesized according to procedure B in 6% yield. MS (ES), *m/z*: 223.2 [M − H]⁻. The title compound (5 mg) was obtained in 52% yield following the general procedure for the Knoevenagel reaction (HPLC: 95.2%, t_R = 3.75 min), mp 319−325 °C. ¹H NMR (DMSO-d_6) δ 12.53 (m, 1H), 10.67 (m, 1H), 7.67 (s, 1H), 7.35 (m, 1H), 7.30 (d, 1H, *J* = 3 Hz), 7.27 (m, 1H), 7.24 (d, 1H, *J* = 3 Hz). MS (ES), *m/z*: 324.2 [M + H]⁺, 322.3 [M − H]⁻. Anal. ($C_{14}H_7F_2NO_4S$) C, H, N.

Crystallization of PI3Kγ and Soaking of Inhibitors. A pVL1393-based vector expressing aa 144-1′102 of human PI3Kγ, in fusion with N-terminal 6 × His-tag, kindly provided by R. Williams (MRC, Cambridge, U.K.), was used for expression in TN5 cells. The protein was purified essentially as described.[12] PI3Kγ, in 20 mM Tris-HCl, pH 7.2, 50 mM (NH_4)$_2SO_4$, 1% betaine, 1% ethylene glycol, 0.02% CHAPS, and 5 mM DTT, was crystallized by sitting drop vapor diffusion. An amount of 5 *μ*L of protein solution was mixed with 5 *μ*L of a solution containing 20−22% PEG 4000, 100 mM Tris-HCl, pH 7.2, and 200 mM (NH_4)$_2SO_4$. Crystals were harvested directly into a soaking solution consisting of 25% PEG 4000, 20 mM (NH_4)$_2SO_4$, 100 mM Tris-HCl, pH 7.2, 10% (v/v) glycerol, and 2 mM of inhibitor and soaked for 24 h. X-ray diffraction data were collected at 100 K at the X06SA beamline at the Swiss Light Source and processed using MOSFLM and programs from the CCP4 package.[51] The atomic models were manually built using O and refined with CNX.[52,53]

pK_a Measurements. Acid−base ionization constants were measured by UV spectroscopy using the GlpKa automatic titrator equipped with the DPAS module (Sirius Ldt, East Sussex, U.K.). The pH electrode was calibrated in the pH range 1.8−12.2 in 0.15

M KCl before use. All titrations were performed under argon atmosphere at 25 ± 0.5 °C. Typically, an amount of 20 *μ*L of 10 mM DMSO stock solution of test sample was dissolved in 15 mL of 0.15 M KCl solutions containing 60, 50, 40, and 30 wt % MeOH prior to titration. Standardized 0.5 M KOH was added to increase the pH to 11.0, and the solutions were titrated with 0.5 M HCl to pH 4. The pH change per titrant addition was limited to 0.15 pH units. After each titrant addition, the pH was measured and the UV spectrum was recorded from 200 to 500 nm. All experiments were carried out in the presence of 0.25 mM potassium dihydrogen phosphate. The data processing, including Yasuda−Shedlovsky extrapolation to cosolvent zero, was carried out using pKaUV software (version 1.001, Sirius Ltd.).

Biological Methods. In Vitro PI3Kγ Lipid Kinase Assay. A PI3Kγ lipid kinase assay, based on the neomycin-coated scintillation proximity assay (SPA) bead technology (Amersham), was performed in 384-well plates using ATP/[γ-³³P]ATP and PtdIns (Sigma) as substrates, as previously described.[10,54] Kinase assays for IC$_{50}$ value determinations with PI3Kα, PI3Kβ, and PI3Kδ were carried out, as previously described.[10]

C5a-Mediated PKB/Akt Phosphorylation in Macrophages. After 3 h of starvation in serum-free medium, Raw-264 macrophages were pretreated with inhibitors or DMSO for 30 min and stimulated for 5 min with 50 nM C5a (Sigma). We monitored PKB/Akt phosphorylation using phospho-Ser-473 Akt specific antibody (CST) and standard ELISA protocols.

MCP-1/CCL2 and CSF-1-Mediated PKB/Akt Phosphorylation in Monocytes. THP-1 monocytes, starved in serum-free medium for 3 h, were pretreated with inhibitors or DMSO for 15 min and stimulated with 100 nM MCP-1/CCL2 (R&D) for 30 s or 50 ng/mL CSF-1 (Peprotec) for 5 min. PKB/Akt phosphorylation was monitored using phospho-Ser-473 Akt specific antibody, as previously described.[10]

SCF-Induced PKB/Akt Phosphorylation in Mast Cells. Primary bone marrow cells were isolated from 4- to 8-week-old wild-type mice as previously described[45] and derived to mast cells by incubation with medium containing 20 ng/mL of stem cell factor (SCF) (PeproTech, Switzerland) and 20 ng/mL of IL-3 (PeproTech, Switzerland) for at least 4 weeks. Confirmation of the expression of mast cell specific surface markers was done by FACS analysis using antibodies against c-kit (cKit-PE mouse antibody, Pharmingen). Cells were maintained in culture in the presence of SCF and IL-3. To induce PKB/Akt phosphorylation, mast cells were resuspended at 2.5 × 10⁶ cells/mL and starved in medium containing no SCF or IL-3 for 24 h. After preincubation with compounds or 1% DMSO for 20 min, cells were activated with 20 ng/mL of SCF for 15 min at 37 °C, fixed in 1.5% paraformaldehyde for 20 min, and permeabilized with 0.2% Triton X-100 for 10 min, at room temperature. PKB/Akt phosphorylation was visualized using phospho-Ser-473 specific Akt antibodies (Cell Signaling) and standard FACS protocols.

Preparation of Mouse Bone Marrow Derived Monocytes (BMDM) and in Vitro Chemotaxis. Bone marrow cells were isolated, prepared, and stimulated, as previously described.[45] For in vitro chemotaxis, 10⁷ 5-day-derived BMDMs were suspended in 1 mL of medium containing 0.5% BSA and inhibitors or DMSO and applied to the upper chamber of a transwell, 5 *μ*m pore size, COSTAR chemotaxis plate. An amount of 600 *μ*L of medium containing MCP-1/CCL2 and inhibitors or DMSO was added to the lower chamber. After 3 h of incubation at 37 °C and 5% CO$_2$, the number of cells in the lower chamber was quantified with a Beckman Coulter AcT 5diffTM.

Computational Methods. Docking. For all modeling studies we used the crystal structure of PI3Kγ in complex with **2**. All docking simulations were performed using the program Glide.[56] The center and the size for for the docking grid box were selected with respect to the cocrystallized ligand, and the default parameters were used. We performed flexible ligand docking using the SP level of accuracy and typically saved five docked poses per ligand for

subsequent analysis. For docking of molecules containing the 2-hydroxy group, a hydrogen-bonding constraint to Val882 NH was requested.

Minimization. Geometry minimization was carried out using the program MacroModel from Schrödinger, LLC, New York. In a typical simulation, a 5 Å shell of completed residues around the ligand was fully minimized using MMFFs and the default settings.

Induced-Fit Docking. The induced-fit docking protocol used is based on docking by Glide and on side chain optimization by Prime (Schrödinger, LLC, New York). We used the default settings, which sampled side chain conformation space of residues within 5 Å from the ligand. Final complex structures were generated by Glide redocking into newly generated protein conformers.

Supporting Information Available: Elemental analysis results for compounds **1**−**14**, **16**−**28**, **30**−**34**, **37**−**41**. This material is available free of charge via the Internet at http://pubs.acs.org.

References

(1) Vanhaesebroeck, B.; Leevers, S. J.; Ahmadi, K.; Timms, J.; Katso, R.; Driscoll, P. C.; Woscholski, R.; Parker, P. J.; Waterfield, M. D. Synthesis and function of 3-phosphorylated inositol lipids. *Annu. Rev. Biochem.* **2001**, *70*, 535−602.

(2) Bi, L.; Okabe, I.; Bernard, D. J.; Wynshaw-Boris, A.; Nussbaum, R. L. Proliferative defect and embryonic lethality in mice homozygous for a deletion in the p110alpha subunit of phosphoinositide 3-kinase. *J. Biol. Chem.* **1999**, *274*, 10963−10968.

(3) Bi, L.; Okabe, I.; Bernard, D. J.; Nussbaum, R. L. Early embryonic lethality in mice deficient in the p110beta catalytic subunit of PI 3-kinase. *Mamm. Genome* **2002**, *13*, 169−172.

(4) Okkenhaug, K.; Bilancio, A.; Farjot, G.; Priddle, H.; Sancho, S.; Peskett, E.; Pearce, W.; Meek, S. E.; Salpekar, A.; Waterfield, M. D.; Smith, A. J.; Vanhaesebroeck, B. Impaired B and T cell antigen receptor signaling in p110delta PI 3-kinase mutant mice. *Science* **2002**, *297*, 1031−1034.

(5) Sasaki, T.; Irie-Sasaki, J.; Jones, R. G.; Oliveira-dos-Santos, A. J.; Stanford, W. L.; Bolon, B.; Wakeham, A.; Itie, A.; Bouchard, D.; Kozieradzki, I.; Joza, N.; Mak, T. W.; Ohashi, P. S.; Suzuki, A.; Penninger, J. M. Function of PI3Kgamma in thymocyte development, T cell activation, and neutrophil migration. *Science* **2000**, *287*, 1040−1046.

(6) Hirsch, E.; Katanaev, V. L.; Garlanda, C.; Azzolino, O.; Pirola, L.; Silengo, L.; Sozzani, S.; Mantovani, A.; Altruda, F.; Wymann, M. P. Central role for G protein-coupled phosphoinositide 3-kinase gamma in inflammation. *Science* **2000**, *287*, 1049−1053.

(7) Li, Z.; Jiang, H.; Xie, W.; Zhang, Z.; Smrcka, A. V.; Wu, D. Roles of PLC-beta2 and -beta3 and PI3Kgamma in chemoattractant-mediated signal transduction. *Science* **2000**, *287*, 1046−1049.

(8) Condliffe, A. M.; Davidson, K.; Anderson, K. E.; Ellson, C. D.; Crabbe, T.; Okkenhaug, K.; Vanhaesebroeck, B.; Turner, M.; Webb, L.; Wymann, M. P.; Hirsch, E.; Ruckle, T.; Camps, M.; Rommel, C.; Jackson, S. P.; Chilvers, E. R.; Stephens, L. R.; Hawkins, P. T. Sequential activation of class IB and class IA PI3K is important for the primed respiratory burst of human but not murine neutrophils. *Blood* **2005,** *106*, 1432−1440.

(9) Laffargue, M.; Calvez, R.; Finan, P.; Trifilieff, A.; Barbier, M.; Altruda, F.; Hirsch, E.; Wymann, M. P. Phosphoinositide 3-kinase gamma is an essential amplifier of mast cell function. *Immunity* **2002,** *16*, 441−451.

(10) Camps, M.; Rückle, T.; Ji, H.; Ardissone, V.; Rintelen, F.; Shaw, J.; Ferrandi, C.; Chabert, C.; Gillieron, C.; Francon, B.; Martin, T.; Gretener, D.; Perrin, D.; Leroy, D.; Vitte, P. A.; Hirsch, E.; Wymann, M. P.; Cirillo, R.; Schwarz, M. K.; Rommel, C. Blockade of PI3Kγ suppresses joint inflammation and damage in mouse models of rheumatoid arthritis. *Nat. Med. (N. Y.)* **2005**, *11*, 936−943.

(11) Wymann, M. P.; Bjoerkloef, K.; Calvez, R.; Finan, P.; Thomast, M.; Trifilieff, A.; Barbier, M.; Altruda, F.; Hirsch, E.; Laffargue, M. Phosphoinositide 3-kinase γ: a key modulator in inflammation and allergy. *Biochem. Soc. Trans.* **2003**, *31*, 275−280.

(12) Walker, E. H.; Pacold, M. E.; Perisic, O.; Stephens, L.; Hawkins, P. T.; Wymann, M. P.; Williams, R. L. Structural determinants of phosphoinositide 3-kinase inhibition by wortmannin, LY294002, quercetin, myricetin, and staurosporine. *Mol. Cell* **2000**, *6*, 909−919.

(13) Gammill, R. B.; Judge, T. M.; Morris, J. Preparation of antiatherosclerotic and antithrombotic 1-benzopyran-4-ones and 2-amino-1,3-benzoxazine-4-ones. PCT Int. Appl. WO9119707, 1991.

(14) Gogliotti, R. D.; Muccioli, K. L.; Para, K. S.; Visnick, M. Preparation of benzoxazines and related compounds as inhibitors of PI3Ks. PCT Int. Appl. WO2004056820, 2004.

(15) Barvian, N. C.; Kolz, C. N.; Para, K. S.; Patt, W. C.; Visnick, M. Preparation of benzoxazin-3-ones and derivatives as inhibitors of PI3K kinase for treating inflammations, cardiovascular diseases and cancers. PCT Int. Appl. WO2004052373, 2004.

(16) Bruendl, M. M.; Connolly, M. K.; Goodman, A. P.; Gogliotti, R. D.; Lee, H. T.; Plummer, M. S.; Sexton, K. E.; Reichard, G. A.; Visnick, M.; Wilson, M. W. Preparation of *N*-tetrazolyl benzo[*b*]-thiophenecarboxamides as phosphoinositide-3-kinase (PI3K) inhibitors for the treatment of cancer, inflammatory and cardiovascular diseases. PCT Int. Appl. WO2004108715, 2004.

(17) Connolly, M. K.; Cogliotti, R. D.; Hurt, C. R.; Reichard, G. A.; Visnick, M. Preparation of halo-substituted *N*-tetrazolylbenzo[*b*]-thiophenecarboxamides with PI3K inhibitory activity as therapeutic agents. PCT Int. Appl. WO2005023800, 2005.

(18) Connolly, M.; Gogliotti, R. D.; Lee, H. T.; Plummer, M. S.; Sexton, K. E.; Visnick, M. Preparation of *N*-tetrazolyl benzo[*b*]thiophenecarboxamides as phosphoinositide-3-kinase (PI3K) inhibitors for the treatment of cancer, inflammatory and cardiovascular diseases. PCT Int. Appl. WO2004108713, 2004.

(19) Gogliotti, R. D.; Lee, H. T.; Sexton, K. E.; Visnick, M. Preparation of tetrazolyl benzofurancarboxamides as phosphoinositide-3-kinase (PI3K) inhibitors for the treatment of cancer, inflammatory and cardiovascular diseases. PCT Int. Appl. WO2004108709, 2004.

(20) Para, K. S.; Stankovic, C. J.; Visnick, M.. Preparation of 3-substituted indoles as inhibitors of phosphoinositide-3 kinases (PI3Ks). PCT Int. Appl. WO2004108708, 2004.

(21) Connolly, M. K.; Gogliotti, R. D.; Plummer, M. S.; Visnick, M. Preparation of morpholinyl-pyrimidine derivatives as inhibitors of phosphoinositide-3-kinases. PCT Int. Appl. WO2005042519, 2005.

(22) Bruce, I.; Finan, P.; Leblanc, C.; McCarthy, C.; Whitehead, L.; Blair, N. E.; Bloomfield, G. C.; Hayler, J.; Kirman, L.; Oza, M. S.; Shukla, L.. 5-Phenylthiazole derivatives and their use as phosphatidylinositol 3-kinase (PI3K) inhibitors for the treatment of allergic and inflammatory diseases. PCT Int. Appl. WO2003072557, 2003.

(23) Shimada, M.; Murata, T.; Fuchikami, K.; Tsujishita, H.; Omori, N.; Kato, I.; Miura, M.; Urbahns, K.; Gantner, F.; Bacon, K. Preparation of fused azole-pyrimidine derivatives as PI3K inhibitors with therapeutic uses. PCT Int. Appl. WO2004029055, 2004.

(24) Bloomfield, G. C.; Bruce, I.; Leblanc, C.; Oza, M. S.; Whitehead, L.. Preparation of 5-phenylthiazoles as phosphatidylinositol 3-kinase (PI3 kinase) inhibitors. PCT Int. Appl. WO2004078754, 2004.

(25) Bruce, I.; Cuenoud, B.; Keller, T. H.; Pilgrim, G. E.; Press, N.; Le Grand, D. M.; Ritchie, C.; Valade, B.; Hayler, J.; Budd, E. Preparation of pyrazinyl/pyridinyl thiazolylamines as inhibitors of phosphatidylinositol 3-kinase. PCT Int. Appl. WO2004096797. 2004.

(26) Bloomfield, G. C.; Bruce, I.; Hayler, J.; Leblanc, C.; Le Grand, D. M.; McCarthy, C. Preparation of phenylthiazolylureas as inhibitors of phosphatidylinositol 3-kinase. PCT Int. Appl. WO2005021519, 2005.

(27) Quattropani, A.; Rückle, T.; Schwarz, M.; Dorbais, J.; Sauer, W.; Cleva, C.; Desforges, G. Preparation of thiazole derivatives as modulators of the phosphoinositide-3-kinases (PI3Ks). PCT Int. Appl. WO2005068444, 2005.

(28) Rückle, T.; Shaw, D.; Church, D.; Covini, D. Preparation of 2-imino-4-(thio)oxo-5-polycyclovinylazolines as PI3 kinase inhibitors. PCT Int. Appl. WO2005011686, 2005.

(29) Rückle, T.; Jiang, X.; Gaillard, P.; Church, D.; Vallotton, T. Preparation of azolidinone-vinyl fused-benzene derivatives for therapeutic uses as PI3 kinase inhibitors. PCT Int. Appl. WO2004007491, 2004.

(30) Robertson, A. D.; Jackson, S.; Kenche, V.; Yaip, C.; Parbaharan, H.; Thompson, P. Preparation and formulation of morpholino-substituted heterocycles as phosphoinositide 3-kinase inhibitors for therapeutic use. PCT Int. Appl. WO2001053266, 2001.

(31) Jackson, S. P.; Robertson, A. D.; Kenche, V.; Thompson, P.; Prabaharan, H.; Anderson, K.; Abbott, B.; Goncalves, I.; Nesbitt, W.; Schoenwaelder, S.; Saylik, D. Preparation of morpholinyl- and pyridinyl-substituted heterobicyclic ketones as selective inhibitors of phosphoinositide-3-kinase β for use against thrombosis. PCT Int. Appl. WO2004016607, 2004.

(32) Cleva, C.; Domine, D.; Merlot, C.; Bunn, J.; Sebille, E.; Sauer, W.; Church, D. Priviledged substructure searching for focused set design. *Abstracts of Papers*, 224th National Meeting of the American Chemical Society, Boston, MA, August 18−22, 2002; American Chemical Society: Washington, DC, 2002.

(33) Church, D.; Colinge, J. Method of operating a computer system to perform a discrete substructural analysis. PCT Int. Appl. WO200233-596, 2002.

(34) Rückle, T.; Grippi-Vallotton, T.; Maio, M.; Covini, D.; Pomel, V.; Burgat-Charvillon, F.; Church, D.; Shaw, J.; Sauer, W.; Klicic, J.; Sherbukhin, V.; Quattropani, A.; Dorbais, J.; Desforges, G.; Valognes, D.; Camps, M.; Chabert, C.; Gillieron, C.; Francon, B.; Perrin, D.; Leroy, D.; Gretener, D.; Nichols, A.; Ji, H.; Rintelen, F.; Ardissone, V.; Ferrandi, C.; Vitte, P. A.; Carboni, S.; Cirillo, R.; Schwarz, M. K.; Rommel, C. Identification and development of azolidinone vinyl-fused benzene derivatives, as potent and selective PI3Kγ inhibitors, orally active in models of rheumatoid arthritis. *Abstracts of Papers*, 230th National Meeting of the American Chemical Society, Washington, DC, August 28 through September 1, 2005; American Chemical Society: Washington, DC, 2005.

(35) Pomel, V.; Klicic J.; Covini, D.; Church, D.; Shaw, J.; Valognes, D.; Camps, M.; Chabert, C.; Gillieron, C.; Françon, B.; Perrin, D.; Leroy, D.; Gretener, D.; Nichols, A.; Vitte, P. A, Carboni, S.; Rommel, C.; Schwarz, M. K.; Rückle, T. Design and synthesis of a novel class of potent and highly isoform selective PI3Kγ inhibitors. *Abstracts of Papers*, 230th National Meeting of the American Chemical Society, Washington, DC, August 28 through September 1, 2005; American Chemical Society: Washington, DC, 2005.

(36) Campbell, I. W. The clinical significance of PPAR gamma agonism. *Curr. Mol. Med.* **2005**, *5*, 349−363.

(37) Yki-Jaervinen, H. Thiazolidinediones. *N. Engl. J. Med.* **2004**, *351*, 1106−1118.

(38) Wiesner, J.; Mitsch, A.; Jomaa, H.; Schlitzer, M. Structure−activity relationships of novel anti-malarial agents. Part 7: *N*-(3-Benzoyl-4-tolylacetylaminophenyl)-3-(5-aryl-2-furyl)acrylic acid amides with polar moieties. *Bioorg. Med. Chem. Lett.* **2003**, *13*, 2159−2161.

(39) Hosoya, T.; Aoyama, H.; Ikemoto, T.; Kihara, Y.; Hiramatsu, T.; Endo, M.; Suzuki, M. Dantrolene analogues revisited: general synthesis and specific functions capable of discriminating two kinds of Ca^{2+} release from sarcoplasmic reticulum of mouse skeletal muscle. *Bioorg. Med. Chem.* **2003**, *11*, 663−673.

(40) Ismail, M. A.; Brun, R.; Wenzler, T.; Tanious, F. A.; Wilson, W. D.; Boykin, D. W. Dicationic biphenyl benzimidazole derivatives as antiprotozoal agents. *Bioorg. Med. Chem. Lett.* **2004**, *12*, 5405−5413.

(41) Chittiboyina, A. G.; Reddy, C.; Watkins, E. B.; Avery, M. A. First synthesis of antimalarial Machaeriols A and B. *Tetrahedron Lett.* **2004**, *45*, 1689−1691.

(42) Dupuis, C.; Adiey, K.; Charruault, L.; Michelet, V.; Savignac, M.; Genet, J. P. Suzuki cross-coupling of arylboronic acids mediated by a hydrosoluble Pd(0)/TPPTS catalyst. *Tetrahedron Lett.* **2001**, *42*, 6523−6526.

(43) Miyaura, N.; Suzuki, A. Palladium-catalyzed cross-coupling reactions of organoboron compounds. *Chem. Rev. (Washington, D.C.)* **1995**, *95*, 2457−2483.

(44) Unangst, P. C.; Connor, D. T.; Cetenko, W. A.; Sorenson, R. J.; Kostlan, C. R.; Sircar, J. C.; Wright, C. D.; Schrier, D. J.; Dyer, R. D. Synthesis and biological evaluation of 5-[[3,5-bis(1,1-dimethyl-ethyl)-4-hydroxyphenyl]methylene]oxazoles, -thiazoles, and -imidazoles: novel dual 5-lipoxygenase and cyclooxygenase inhibitors with antiinflammatory activity. *J. Med. Chem.* **1994**, *37*, 322−328.

(45) Weiss-Haljiti, C.; Pasquali, C.; Ji, H.; Gillieron, C.; Chabert, C.; Curchod, M. L.; Hirsch, E.; Ridley, A. J.; van Huijsduijnen, R. H.; Camps, M.; Rommel, C. Involvement of phosphoinositide 3-kinase gamma, Rac, and PAK signaling in chemokine-induced macrophage migration. *J. Biol. Chem.* **2004**, *279*, 43273−43284.

(46) Okkenhaug, K.; Bilancio, A.; Farjot, G.; Priddle, H.; Sancho, S.; Peskett, E.; Pearce, W.; Meek, S. E.; Salpekar, A.; Waterfield, M. D.; Smith Andrew, J. H.; Vanhaesebroeck, B. Impaired B and T cell antigen receptor signaling in p110delta PI 3-kinase mutant mice. *Science* **2002**, *297*, 1031−1034.

(47) Jones, G. E.; Prigmore, E.; Calvez, R.; Hogan, C.; Dunn, G. A.; Hirsch, E.; Wymann, M. P.; Ridley, A. J. Requirement for PI 3-kinase gamma in macrophage migration to MCP-1 and CSF-1. *Exp. Cell Res.* **2003**, *290*, 120−131.

(48) Johnson, Z.; Power, C. A.; Weiss, C.; Rintelen, F.; Ji, H.; Ruckle, T.; Camps, M.; Wells, T. N. C.; Schwarz, M. K.; Proudfoot, A. E. I.; Rommel, C. Chemokine inhibition—why, when, where, which and how? *Biochem. Soc. Trans.* **2004**, *32*, 366−377.

(49) Schwarz, M. K.; Wells, T. N. New therapeutics that modulate chemokine networks. *Nat. Rev. Drug Discovery* **2002**, *1*, 347−58.

(50) Henderson, R. B.; Hobbs, J. A.; Mathies, M.; Hogg, N. Rapid recruitment of inflammatory monocytes is independent of neutrophil migration. *Blood* **2003**, *102*, 328−335.

(51) Leslie, A. G. Integration of macromolecular diffraction data. *Acta Crystallogr.* **1999**, *D55*, 1696−1702.

(52) Jones, T. A.; Zou, J. Y.; Cowan, S. W.; Kjeldgaard, M. Improved methods for building protein models in electron density maps and the location of errors in these models. *Acta Crystallogr.* **1991**, *A47*, 110−119.

(53) Brunger, A. T.; Adams, P. D.; Clore, G. M.; DeLano, W. L.; Gros, P.; Grosse-Kunstleve, R. W.; Jiang, J. S.; Kuszewski, J.; Nilges, M.; Pannu, N. S.; Read, R. J.; Rice, L. M.; Simonson, T.; Warren, G. L. Crystallography & NMR system: A new software suite for macro-molecular structure determination. *Acta Crystallogr., Sect. D.: Biol. Crystallogr.* **1998**, *54*, 905−921.

(54) Camps, M.; Chabert, C.; Martin, T.; Perrin, D.; Rommel, C.; Wymann, M. P. Use of a scintillating solid support coated with an aminoglycoside for identifying and/or quantifying a radiolabeled aminoglycoside binding molecule such as mono- or polyphosphated phosphoinositide in a sample. PCT Int. Appl. WO2002101084, 2002.

(55) Chatham, W. W.; Swaim, R.; Frohsin, H., Jr.; Heck, L. W.; Miller, E. J.; Blackburn, W. D., Jr. Degradation of human articular cartilage by neutrophils in synovial fluid. *Arthritis Rheum.* **1993**, *36*, 51−58.

(56) Friesner, R. A.; Banks, J. L.; Murphy, R. B.; Halgren, T. A.; Klicic, J. J.; Mainz, D. T.; Repasky, M. P.; Knoll, E. H.; Shelley, M.; Perry, J. K.; Shaw, D. E.; Francis, P.; Shenkin, P. S. Glide: A new approach for rapid, accurate docking and scoring. 1. method and assessment of docking accuracy. *J. Med. Chem.* **2004**, *47*, 1739−1749.

(57) Sadhu, C.; Dick, K.; Treiberg, K.; Sowell, G.; Kesicki, E.; Oliver, A. Inhibitors of human phosphatidyl-inositol 3-kinase delta. PCT Int. Appl. WO200181346, 2001.

(58) Breitfelder, S.; Maier, U.; Grauert, M.; Brandl, T.; Hoffmann, M.; Hoenke, C.; Pautsch, A.; Kalkbrenner, F.; Joergensen, A.; Schaenzle, G.; Peters, S.; Buettner, F.; Bauer, E. PI3 kinases. PCT Int. Appl. WO2006040279, 2006.